AIMS Mathematics, 9(1): 340–370.
DOI:10.3934/math.2024020
Received: 09 August 2023
Revised: 29 September 2023
Accepted: 12 October 2023
Published: 29 November 2023

http://www.aimspress.com/journal/Math

*Research article*

# On numerical solution of two-dimensional variable-order fractional diffusion equation arising in transport phenomena

**Fouad Mohammad Salama*** **and Faisal Fairag**

Department of Mathematics, King Fahd University of Petroleum & Minerals, Dhahran, Saudi Arabia

* **Correspondence:** Email: fuadmohd321@gmail.com.

**Abstract:** In recent years, the application of variable-order (VO) fractional differential equations for describing complex physical phenomena ranging from biology, hydrology, mechanics and viscoelasticity to fluid dynamics has become one of the most hot topics in the context of scientific modeling. An interesting aspect of VO operators is their capability to address the behavior of scientific and engineering systems with time and spatially varying properties. The VO fractional diffusion equation is a fundamental model that allows transitions among sub-diffusive, diffusive and super-diffusive behaviors without altering the underlying governing equations. In this paper, we considered the two-dimensional fractional diffusion equation with the Caputo time VO derivative, which is essential for describing anomalous diffusion in real-world complex systems. A new Crank-Nicolson (C-N) difference scheme and an efficient explicit decoupled group (EDG) method were proposed to solve the problem under consideration. The proposed EDG method is based on a skewed difference scheme in conjunction with a grouping procedure of the solution grid points. Special attention was devoted to investigating the stability and convergence of the proposed methods. Three numerical examples with known exact analytical solutions were provided to illustrate our considerations. The proposed methods were shown to be stable and convergent theoretically as well as numerically. In addition, a comparative study was done between the EDG method and the C-N difference scheme. It was found that the proposed methods are accurate in simulating the considered problem, while the EDG method is superior to the C-N difference method in terms of Central Processing Unit (CPU) timing, verifying the efficiency of the former method in solving the VO problem.

**Keywords:** fractional diffusion equation; variable-order; Crank-Nicolson (C-N) scheme; explicit decoupled group method; stability and convergence; numerical simulation
**Mathematics Subject Classification:** 35R11, 65M06, 65M12

**Nomenclature**

VO: Variable-order.
CO: Constant-order.
C-N: Crank-Nicolson.
EDG: Explicit decoupled group.
CPU: Central processing unit.
VO-TFDE: Variable-order time fractional diffusion equation.

**Symbols**

$M_1$: Number of spatial steps in the $x$-direction.
$M_2$: Number of spatial steps in the $y$-direction.
$N$: Number of temporal steps.
$\Delta x$: Length of spatial step along $x$-direction.
$\Delta y$: Length of spatial step along $y$-direction.
$\tau$: Temporal step size.
$T$: Final time.
$K_1$: Diffusion coefficient.
$K_2$: Diffusion coefficient.
$\alpha$: Fractional order.

## 1. Introduction

A plethora of problems in engineering applications can be described by integer-order differential equations [1]. On the other hand, fractional differential equations have numerous applications in many sciences, which makes them one of the most prominent tools of fractional calculus that have attracted the interest of scholars and researchers in recent years. For instance, Lozynskyy et al. [2] applied the Caputo-Fabrizio operator to describe the elastic moment in a long shaft and produced an enhanced mathematical model in the form of a fractional ordinary differential equation for a two-mass system with concentrated parameters. Asjad et al. [3] successfully described the convection heat transfer in clay nanofluid by utilizing a Maxwell model. The authors used the newly developed hybrid fractional derivative in [4] to generalize the classical Maxwell model to the novel fractional one. Liu et al. [5] established a new Green-Ampt model containing a Caputo fractional derivative to describe an important phenomenon in geotechnical engineering; that is, the infiltration process in slopes. The researchers argued that the outcomes of their model were better than those of Chen and Young's model and very close to the actual experimental results. Kumar et al. [6] provided an opportunity for a better understanding of climate change by introducing a fractional-order model that describes the plankton-oxygen dynamics based on the Liouville-Caputo fractional derivative. Mustafa Inc et al. [7] considered a novel Covid-19 model based on the Caputo fractional operator to study the dynamics of the disease spread. The results of the numerical simulations were in good match with the real data and showed the advantages of the fractional derivative. Shen et al. [8] got more insight into the case where a patient

has two infections at the same time by considering a fractional co-infection model under the Caputo fractional derivative.

Differential equations with constant-order (CO) fractional derivatives have been considered as powerful instruments for characterizing the long memory of dynamic processes and real-world phenomena. This means modeling the case in which the current state of the system depends on all its historical states rather than only some recent ones. More theoretical and comprehensive discussions of fractional calculus can be found in [9–14]. In recent years, many researchers have found systems exhibiting variable memory that cannot be described adequately by CO fractional operators. This fact led to the generalization of the CO fractional calculus to the so-called variable-order (VO) fractional calculus, where the derivatives of fractional operators are functions of time and/or space variables. Sun et al. [15] introduced an important comparative study between constant and VO operators in describing the memory property of systems. It was Samko and Ross [16] who gave the definitions of VO derivatives for the first time in 1993. Later, Lorenzo and Hartley [17, 18] and Coimbra [19] constructed the mathematical framework of VO operators and discussed some of their potential applications in mechanics. These works paved the way for the development of new definitions, which served as a springboard for the field of VO fractional calculus. The list of the definitions in the literature includes: Riemann-Liouville, Caputo, Grunwald-Letnikov, Hadamard, Caputo-Fabrizio, Atangana-Baleanu and more. These definitions are reported to describe complex dynamic problems effectively. Consequently, with the extension of CO fractional models to their counterparts, VO models have grown in a remarkable manner. Examples are the diffusion equation [20], reaction-diffusion equation [21], Burgers equation citer21, telegraph equation [23], mobile/immobile equation [24], Schrödinger equation [25] and more. For more details about the VO fractional calculus, the interested reader is referred to [26–28].

In the last few years, VO fractional differential equations have achieved tremendous success in modeling physical problems of evolutionary nature-type. The reason for this is the ability of VO operators to adjust the system's order based on its present or even its previous response effectively. For example, Sweilam et al. [29] proposed a VO fractional model to simulate the healing process of the cancer disease in biological systems. The established model involved VO Caputo derivatives with two control variables to reduce the number of cancer cells. Xiang and others [30] made use of the VO Caputo derivative and came up with a novel fractional model for describing the stress responses of glassy polymers. The authors noticed a relationship between the varying order and the behavior of microstructures, which opens up a new avenue for manufacturing new polymers with enhanced properties. Liu et al. [31] suggested a fractional damage creep model to depict the mechanical behavior of creep, i.e., the time-dependent behavior under constant stress. Their model relied on the Caputo derivative of the VO function, which is related to the relaxation time of the rheological model. In another study, Fei et al. [32] developed a Maxwell model with VO fractional derivative to describe the creep phenomenon of a salt rock. A fractional model with a VO time derivative for an economic system was proposed and analyzed in [33]. Fan et al. [34] constructed a VO fractional model and showed its superiority over the Anand model in reporting the mechanical properties of sintered nano-silver particles. To get more insight into the applications of VO fractional calculus, the interested reader is referred to the valuable works [35, 36].

Fractional diffusion equations are among the most important models of fractional calculus that are applied to describe the anomalous diffusion phenomena in complex systems. Until date, a plethora

of numerical methods have been developed to handle the diffusion models with CO fractional derivatives [37–46]. However, real data has revealed that the mean square displacement scales as a function of time and/or space variables, which cannot be characterized by CO fractional diffusion models [35]. As a result, fractional diffusion equations with variable orders were introduced to deal with the aforementioned issue. It is worth mentioning that solving variable-order fractional diffusion equations analytically is highly complex and cannot be achieved in many cases due to the variable exponent. This stimulated numerical researchers to design efficient approximation methods for solving these equations, namely, finite difference methods [47–49], finite element methods [20, 50], wavelet methods [51], collocation methods [52, 53], reproducing kernel methods [54] and others.

Due to the nonlocal property of VO operators, standard numerical schemes lead to costly simulations, particularly when a high-dimensional problem or mesh refinement is considered. Explicit group difference methods are combinations of finite difference schemes and grouping strategies on standard and skewed grids. In fact, explicit group difference methods can efficiently reduce the spectral radius of the iteration matrix and increase the convergence rates of the approximation methods. Besides, these methods can be implemented on parallel computers, which makes them very advantageous in practice. In the past few years, several researchers have successfully extended the explicit group difference methods from solving integer-order differential equations to handling various types of CO fractional differential equations [55–60]. For more details, the interested reader can refer to the cited studies. However, to the best of our knowledge, there have been no trials to utilize explicit group difference methods to determine numerical solutions of differential equations in the frame of VO fractional derivatives. In this line of reasoning, this article aims to provide a grouping-based numerical method to deal with the two-dimensional VO time fractional diffusion equation (VO-TFDE) of the following form:

$$\begin{cases} {}_0^C D_t^{\alpha(x,y,t)} u(x,y,t) = K_1 \dfrac{\partial^2 u(x,y,t)}{\partial x^2} + K_2 \dfrac{\partial^2 u(x,y,t)}{\partial y^2} + f(x,y,t), \ (x,y,t) \in \Omega \times (0,T], & (1.1) \\ u(x,y,t) = h(x,y,t), \quad (x,y,t) \in \partial\Omega \times (0,T], & (1.2) \\ u(x,y,0) = g(x,y), \quad (x,y) \in \Omega \cup \partial\Omega, & (1.3) \end{cases}$$

where $\Omega = [0, L] \times [0, L]$ is a closed subset in $\mathbb{R}^2$ representing the solution domain, $\partial\Omega$ is its boundary, $K_1$ and $K_2$ are positive constants denoting the diffusion coefficients, $f(x, y, t)$, $h(x, y, t)$ and $g(x, y)$ are known smooth functions and $u(x, y, t)$ is the unknown function. $0 < \alpha(x, y, t) < 1$, ${}_0^C D_t^{\alpha(x,y,t)} u(x, y, t)$ is the VO Caputo derivative defined as

$${}_0^C D_t^{\alpha(x,y,t)} u(x,y,t) = \begin{cases} \frac{1}{\Gamma(1-\alpha(x,y,t))} \int_0^t (t-\xi)^{-\alpha(x,y,t)} \frac{\partial u(x,y,\xi)}{\partial \xi} d\xi, \ 0 < \alpha(x,y,t) < 1, \\ \frac{\partial u(x,y,t)}{\partial t}, \ \alpha(x,y,t) = 1. \end{cases}$$

The above definition of the Caputo derivative has received a great deal of interest in the field of applications since it allows the traditional initial and boundary conditions that have solid physical interpretations to be imposed in the fractional models. The aim of this study is to construct a new grouping-based numerical method, namely, the explicit decoupled group (EDG) method for the two-dimensional VO-TFDE (1.1). We start by introducing a Crank-Nicolson (C-N) finite difference method, which serves as a reference scheme to examine the efficiency of the proposed method. Thereafter, the EDG method is developed based on a new difference scheme that is derived by rotating

the standard grid and applying the Taylor series expansion. The resulting method is computationally advantageous since it considers only half of the mesh points in the iteration process at each time level, which means the numerical solutions can be computed in a short time. The stability, convergence and numerical implementations of the proposed methods are also presented in this work. As far as we know, explicit group difference methods with stability and convergence analyses for VO fractional models have not appeared in the literature.

The rest of this paper is as follows: The next section presents a C-N finite difference scheme to solve the two-dimensional VO-TFDE (1.1). In section three, we propose the EDG method for the mentioned equation. The stability and convergence analyses are included in sections four and five, respectively. Some numerical experiments are reported in section six to validate the efficiency and accuracy of the presented methods. Finally, a brief conclusion is expressed in section seven.

## 2. The C-N difference scheme

In this section, we present a C-N numerical scheme for solving the VO-TFDE (1.1). Such a discretization scheme will reduce the considered problem into a system of simultaneous algebraic equations, which can be solved by a proper numerical technique. To this end, we let $x_i = i\Delta x$, $0 \le i \le M_1$, $y_j = j\Delta y$, $0 \le j \le M_2$, $t_k = k\tau$, $0 \le k \le N$, where $M_1$, $M_2$ and $N$ are some positive integers. Here, $\Delta x = L/M_1$, $\Delta y = L/M_2$ and $\tau = T/N$ represent the spatial and temporal step sizes, respectively. For simplicity, define $u_{i,j}^k$ as the numerical approximation at the point $(x_i, y_j, t_k)$ and $f(x_i, y_j, t_k) = f_{i,j}^k$. Then, the discretization of the second order space derivatives is expressed as:

$$\begin{aligned}\frac{\partial^2 u(x_i, y_j, t_{k+1/2})}{\partial x^2} &= \frac{1}{2}\left[\frac{u_{i+1,j}^{k+1} - 2u_{i,j}^{k+1} + u_{i-1,j}^{k+1}}{(\Delta x)^2} + \frac{u_{i+1,j}^{k} - 2u_{i,j}^{k} + u_{i-1,j}^{k}}{(\Delta x)^2}\right] \\ &\quad + O(\tau^2 + (\Delta x)^2) + (\Delta y)^2), \qquad (2.1)\\ \frac{\partial^2 u(x_i, y_j, t_{k+1/2})}{\partial y^2} &= \frac{1}{2}\left[\frac{u_{i,j+1}^{k+1} - 2u_{i,j}^{k+1} + u_{i,j-1}^{k+1}}{(\Delta y)^2} + \frac{u_{i,j+1}^{k} - 2u_{i,j}^{k} + u_{i,j-1}^{k}}{(\Delta y)^2}\right] \\ &\quad + O(\tau^2 + (\Delta x)^2) + (\Delta y)^2). \qquad (2.2)\end{aligned}$$

For the approximation of the Caputo time VO derivative, we utilize the following discretization scheme [61]:

$$\begin{aligned}&{}_0^C D_t^{\alpha^{i,j,k+1/2}} u(x_i, y_j, t_{k+1/2}) \\ &= \sigma^{i,j,k}\left[\mathcal{W}_1^{i,j,k} u_{i,j}^k - \sum_{s=1}^{k-1}\left(\mathcal{W}_{k-s}^{i,j,k} - \mathcal{W}_{k-s+1}^{i,j,k}\right) u_{i,j}^s - \mathcal{W}_k^{i,j,k} u_{i,j}^0 + \frac{u_{i,j}^{k+1} - u_{i,j}^k}{2^{1-\alpha^{i,j,k+1/2}}}\right] \qquad (2.3)\\ &+ r^{k+1/2},\end{aligned}$$

where $0 < \alpha(x, y, t) < 1$, $\alpha^{i,j,k+1/2} = \alpha(x_i, y_j, t_{k+1/2})$ and

$$\begin{aligned}\sigma^{i,j,k} &= \frac{1}{\Gamma(2 - \alpha^{i,j,k+1/2})\tau^{\alpha^{i,j,k+1/2}}},\\ \mathcal{W}_s^{i,j,k} &= (s + 1/2)^{1-\alpha^{i,j,k+1/2}} - (s - 1/2)^{1-\alpha^{i,j,k+1/2}}.\end{aligned}$$

The local error term has the following bound,

$$|r^{k+1/2}| \leq C\tau.$$

Now, setting Eqs (2.1), (2.2) and (2.3) into (1.1), we get the following,

$$\begin{aligned}
&\sigma^{i,j,k}\left[\mathcal{W}_1^{i,j,k}u_{i,j}^k - \sum_{s=1}^{k-1}\left(\mathcal{W}_{k-s}^{i,j,k} - \mathcal{W}_{k-s+1}^{i,j,k}\right)u_{i,j}^s - \mathcal{W}_k^{i,j,k}u_{i,j}^0 + \frac{u_{i,j}^{k+1} - u_{i,j}^k}{2^{1-\alpha^{i,j,k+1/2}}}\right] \\
&= \frac{K_1}{2}\left[\frac{u_{i+1,j}^{k+1} - 2u_{i,j}^{k+1} + u_{i-1,j}^{k+1}}{(\Delta x)^2} + \frac{u_{i+1,j}^{k} - 2u_{i,j}^{k} + u_{i-1,j}^{k}}{(\Delta x)^2}\right] \\
&+ \frac{K_2}{2}\left[\frac{u_{i,j+1}^{k+1} - 2u_{i,j}^{k+1} + u_{i,j-1}^{k+1}}{(\Delta y)^2} + \frac{u_{i,j+1}^{k} - 2u_{i,j}^{k} + u_{i,j-1}^{k}}{(\Delta y)^2}\right] \\
&+ f_{i,j}^{k+1/2} + O(\tau + (\Delta x)^2) + (\Delta y)^2).
\end{aligned} \tag{2.4}$$

By omitting the local error terms and replacing $u_{i,j}^k$ with its approximation $\mathfrak{U}_{i,j}^k$, the desired result of the C-N difference scheme is obtained as

$$\begin{cases}
(\mathfrak{A}^{i,j,k} + 2\mathfrak{B}_1 + 2\mathfrak{B}_2)\mathfrak{U}_{i,j}^{k+1} = \mathfrak{B}_1(\mathfrak{U}_{i+1,j}^{k+1} + \mathfrak{U}_{i-1,j}^{k+1} + \mathfrak{U}_{i+1,j}^{k} + \mathfrak{U}_{i-1,j}^{k}) \\
+\mathfrak{B}_2(\mathfrak{U}_{i,j+1}^{k+1} + \mathfrak{U}_{i,j-1}^{k+1} + \mathfrak{U}_{i,j+1}^{k} + \mathfrak{U}_{i,j-1}^{k}) + (\mathfrak{A}^{i,j,k} - \sigma^{i,j,k}W_1^{i,j,k} - 2\mathfrak{B}_1 - 2\mathfrak{B}_2)\mathfrak{U}_{i,j}^{k} \\
+\sigma^{i,j,k}\sum_{s=1}^{k-1}\left(\mathcal{W}_{k-s}^{i,j,k} - \mathcal{W}_{k-s+1}^{i,j,k}\right)\mathfrak{U}_{i,j}^{s} + \sigma^{i,j,k}\mathcal{W}_k^{i,j,k}\mathfrak{U}_{i,j}^0 + f_{i,j}^{k+1/2}, \\
1 \leq i \leq M_1 - 1,\ 1 \leq j \leq M_2 - 1,\ 0 \leq k \leq N - 1, \\
\mathfrak{A}^{i,j,k} = \frac{\sigma^{i,j,k}}{2^{1-\alpha^{i,j,k+1/2}}},\ \mathfrak{B}_1 = \frac{K_1}{2(\Delta x)^2},\ \mathfrak{B}_2 = \frac{K_2}{2(\Delta y)^2}. \\
\text{The initial and boundary conditions are} \\
\mathfrak{U}_{i,j}^0 = g(x_i, y_j),\ 0 \leq i \leq M_1,\ 0 \leq j \leq M_2, \\
\mathfrak{U}_{i,j}^k|_{\partial\Omega} = h(x_i, y_j, t_k),\ 0 \leq k \leq N.
\end{cases} \tag{2.5}$$

Let

$$\begin{aligned}
U^k &= [\mathfrak{U}_{1,1}, \mathfrak{U}_{1,2}, \ldots, \mathfrak{U}_{1,M_2-1}, \mathfrak{U}_{2,1}, \mathfrak{U}_{2,2}, \ldots, \mathfrak{U}_{2,M_2-1}, \ldots, \mathfrak{U}_{M_1-1,1}, \mathfrak{U}_{M_1-1,2}, \ldots, \mathfrak{U}_{M_1-1,M_2-1}]^T, \\
f^k &= [f_{1,1}, f_{1,2}, \ldots, f_{1,M_2-1}, f_{2,1}, f_{2,2}, \ldots, f_{2,M_2-1}, \ldots, f_{M_1-1,1}, f_{M_1-1,2}, \ldots, f_{M_1-1,M_2-1}]^T.
\end{aligned}$$

The above difference scheme can be represented in matrix form as,

$$\begin{cases}
AU^1 = BU^0 + f^{1/2},\ k = 0, \\
AU^{k+1} = BU^k + \sigma\sum_{m=1}^{k-1}\left(\mathcal{W}_{k-m}\mathcal{W}_{k-m+1}\right)U^m + \sigma\mathcal{W}_kU^0 + f^k,\ k \geq 1.
\end{cases}$$

Here, $A$ and $B$ are pentadiagonal matrices given by

$$A = \begin{bmatrix} \mathfrak{M}^{i,j,k} & \dots & -\mathfrak{B}_1 & \dots & -\mathfrak{B}_2 & \dots & & 0 \\ \vdots & \mathfrak{M}^{i,j,k} & \dots & -\mathfrak{B}_1 & \dots & -\mathfrak{B}_2 & & \vdots \\ -\mathfrak{B}_1 & \ddots & \mathfrak{M}^{i,j,k} & \ddots & \ddots & & \ddots & \\ \vdots & \ddots & \ddots & \ddots & & & \ddots & -\mathfrak{B}_2 \\ -\mathfrak{B}_2 & & -\mathfrak{B}_1 & \ddots & \ddots & & \ddots & \vdots \\ \vdots & -\mathfrak{B}_2 & \ddots & \ddots & & \ddots & & -\mathfrak{B}_1 \\ & & \ddots & & \ddots & & \ddots & \vdots \\ 0 & \dots & & -\mathfrak{B}_2 & \dots & -\mathfrak{B}_1 & \dots & \mathfrak{M}^{i,j,k} \end{bmatrix},$$

$$B = \begin{bmatrix} \mathfrak{N}^{i,j,k} & \dots & \mathfrak{B}_1 & \dots & \mathfrak{B}_2 & \dots & & 0 \\ \vdots & \mathfrak{N}^{i,j,k} & \dots & \mathfrak{B}_1 & \dots & \mathfrak{B}_2 & & \vdots \\ \mathfrak{B}_1 & \ddots & \mathfrak{N}^{i,j,k} & \ddots & \ddots & & \ddots & \\ \vdots & \ddots & \ddots & \ddots & & & \ddots & \mathfrak{B}_2 \\ \mathfrak{B}_2 & & \mathfrak{B}_1 & \ddots & \ddots & & \ddots & \vdots \\ \vdots & \mathfrak{B}_2 & \ddots & \ddots & & \ddots & & \mathfrak{B}_1 \\ & & \ddots & & \ddots & & \ddots & \vdots \\ 0 & \dots & & \mathfrak{B}_2 & \dots & \mathfrak{B}_1 & \dots & \mathfrak{N}^{i,j,k} \end{bmatrix},$$

where

$$\mathfrak{M}^{i,j,k} = \mathfrak{A}^{i,j,k} + 2\mathfrak{B}_1 + 2\mathfrak{B}_2,\ \mathfrak{N}^{i,j,k} = \mathfrak{A}^{i,j,k} - \sigma^{i,j,k}\mathcal{W}_1^{i,j,k} - 2\mathfrak{B}_1 - 2\mathfrak{B}_2.$$

From the structure of the above matrices, it's evident that the matrix $A$ is a strictly diagonally dominant matrix. Hence, we deduce that the C-N difference scheme (2.5) is uniquely solvable. In the next section, the EDG method is proposed.

## 3. The fractional EDG method

The EDG method was first introduced by Abdullah [62] as an efficient and reliable Poisson solver. The success of the EDG technique in handling the Poisson equation has initiated interest in its application to solving various types of differential equations under the frame of integer-order and CO fractional derivatives. Here, we extend the formulation of the EDG method for solving the two-dimensional VO-TFDE (1.1). In this endeavor, another discretization scheme derived by rorating the standard grid 45 clockwise is necessitated to approximate Eq (1.1). Thus, the rotated C-N finite

difference approximation can be written as follows,

$$\begin{aligned}
&\sigma^{i,j,k}\Big[\mathcal{W}_1^{i,j,k}u_{i,j}^k - \sum_{s=1}^{k-1}\left(\mathcal{W}_{k-s}^{i,j,k} - \mathcal{W}_{k-s+1}^{i,j,k}\right)u_{i,j}^s - \mathcal{W}_k^{i,j,k}u_{i,j}^0 + \frac{u_{i,j}^{k+1} - u_{i,j}^k}{2^{1-\alpha^{i,j,k+1/2}}}\Big] \\
&= \frac{K_1}{2}\left[\frac{u_{i+1,j-1}^{k+1} - 2u_{i,j}^{k+1} + u_{i-1,j+1}^{k+1}}{2(\Delta x)^2} + \frac{u_{i+1,j-1}^{k} - 2u_{i,j}^{k} + u_{i-1,j+1}^{k}}{2(\Delta x)^2}\right] \\
&+ \frac{K_2}{2}\left[\frac{u_{i+1,j+1}^{k+1} - 2u_{i,j}^{k+1} + u_{i-1,j-1}^{k+1}}{2(\Delta y)^2} + \frac{u_{i+1,j+1}^{k} - 2u_{i,j}^{k} + u_{i-1,j-1}^{k}}{2(\Delta y)^2}\right] \\
&+ f_{i,j}^{k+1/2} + O(\tau + (\Delta x)^2) + (\Delta y)^2).
\end{aligned} \tag{3.1}$$

By dropping the local error terms and replacing $u_{i,j}^k$ with its approximation $\mathfrak{U}_{i,j}^k$, the following expression is obtained,

$$\begin{aligned}
&(\mathfrak{A}^{i,j,k} + 2\mathfrak{C}_1 + 2\mathfrak{C}_2)\mathfrak{U}_{i,j}^{k+1} = \mathfrak{C}_1(\mathfrak{U}_{i+1,j-1}^{k+1} + \mathfrak{U}_{i-1,j+1}^{k+1} + \mathfrak{U}_{i+1,j-1}^{k} + \mathfrak{U}_{i-1,j+1}^{k}) \\
&+ \mathfrak{C}_2(\mathfrak{U}_{i+1,j+1}^{k+1} + \mathfrak{U}_{i-1,j-1}^{k+1} + \mathfrak{U}_{i+1,j+1}^{k} + \mathfrak{U}_{i-1,j-1}^{k}) + (\mathfrak{A}^{i,j,k} - \sigma^{i,j,k}W_1^{i,j,k} - 2\mathfrak{C}_1 - 2\mathfrak{C}_2)\mathfrak{U}_{i,j}^{k} \\
&+ \sigma^{i,j,k}\sum_{s=1}^{k-1}\left(\mathcal{W}_{k-s}^{i,j,k} - \mathcal{W}_{k-s+1}^{i,j,k}\right)\mathfrak{U}_{i,j}^{s} + \sigma^{i,j,k}\mathcal{W}_k^{i,j,k}\mathfrak{U}_{i,j}^{0} + f_{i,j}^{k+1/2},
\end{aligned} \tag{3.2}$$

where $\mathfrak{C}_g = K_1/(4(\Delta x)^2)$ and $\mathfrak{C}_y = K_2/(4(\Delta y)^2)$.

Consider the location points $(i, j)$, $(i+1, j+1)$, $(i+1, j)$ and $(i, j+1)$. The application of Eq (3.2) to any group of these four points will lead to the $(4 \times 4)$ system of equation represented in the following matrix form (see [62] for extra details),

$$\begin{bmatrix} \mathfrak{D}_1 & -\mathfrak{C}_2 & 0 & 0 \\ -\mathfrak{C}_2 & \mathfrak{D}_2 & 0 & 0 \\ 0 & 0 & \mathfrak{D}_3 & -\mathfrak{C}_1 \\ 0 & 0 & -\mathfrak{C}_1 & \mathfrak{D}_4 \end{bmatrix}\begin{bmatrix} \mathfrak{U}_{i,j}^{k+1} \\ \mathfrak{U}_{i+1,j+1}^{k+1} \\ \mathfrak{U}_{i+1,j}^{k+1} \\ \mathfrak{U}_{i,j+1}^{k+1} \end{bmatrix} = \begin{bmatrix} rhs_{i,j} \\ rhs_{i+1,j+1} \\ rhs_{i+1,j} \\ rhs_{i,j+1} \end{bmatrix}, \tag{3.3}$$

where

$$\begin{aligned}
&\mathfrak{D}_1 = \mathfrak{A}^{i,j,k} + 2\mathfrak{C}_1 + 2\mathfrak{C}_2,\ \mathfrak{D}_2 = \mathfrak{A}^{i+1,j+1,k} + 2\mathfrak{C}_1 + 2\mathfrak{C}_2, \\
&\mathfrak{D}_3 = \mathfrak{A}^{i+1,j,k} + 2\mathfrak{C}_1 + 2\mathfrak{C}_2,\ \mathfrak{D}_4 = \mathfrak{A}^{i,j+1,k} + 2\mathfrak{C}_1 + 2\mathfrak{C}_2,
\end{aligned}$$

and

$$\begin{aligned}
rhs_{i,j} =& \mathfrak{C}_1(\mathfrak{U}_{i+1,j-1}^{k+1} + \mathfrak{U}_{i-1,j+1}^{k+1} + \mathfrak{U}_{i+1,j-1}^{k} + \mathfrak{U}_{i-1,j+1}^{k}) + \mathfrak{C}_2(\mathfrak{U}_{i-1,j-1}^{k+1} \\
&+ \mathfrak{U}_{i+1,j+1}^{k} + \mathfrak{U}_{i-1,j-1}^{k}) + (\mathfrak{A}^{i,j,k} - \sigma^{i,j,k}\mathcal{W}_1^{i,j,k} - 2\mathfrak{C}_1 - 2\mathfrak{C}_2)\mathfrak{U}_{i,j}^{k} \\
&+ \sigma^{i,j,k}\sum_{s=1}^{k-1}\left(\mathcal{W}_{k-s}^{i,j,k} - \mathcal{W}_{k-s+1}^{i,j,k}\right)\mathfrak{U}_{i,j}^{s} + \sigma^{i,j,k}\mathcal{W}_k^{i,j,k}\mathfrak{U}_{i,j}^{0} + f_{i,j}^{k+1/2}, \\
rhs_{i+1,j+1} =& \mathfrak{C}_1(\mathfrak{U}_{i+2,j}^{k+1} + \mathfrak{U}_{i,j+2}^{k+1} + \mathfrak{U}_{i+2,j}^{k} + \mathfrak{U}_{i,j+2}^{k}) + \mathfrak{C}_2(\mathfrak{U}_{i+2,j+2}^{k+1} + \mathfrak{U}_{i+2,j+2}^{k} \\
&+ \mathfrak{U}_{i,j}^{k}) + (\mathfrak{A}^{i+1,j+1,k} - \sigma^{i,j,k}\mathcal{W}_1^{i+1,j+1,k} - 2\mathfrak{C}_1 - 2\mathfrak{C}_2)\mathfrak{U}_{i+1,j+1}^{k}
\end{aligned}$$

$$
\begin{aligned}
&+\sigma^{i+1,j+1,k}\sum_{s=1}^{k-1}\left(\mathcal{W}_{k-s}^{i+1,j+1,k}-\mathcal{W}_{k-s+1}^{i+1,j+1,k}\right)\mathfrak{U}_{i+1,j+1}^{s}\\
&+\sigma^{i+1,j+1,k}\mathcal{W}_{k}^{i+1,j+1,k}\mathfrak{U}_{i+1,j+1}^{0}+f_{i+1,j+1}^{k+1/2},\\
rhs_{i+1,j}=&\mathfrak{C}_1(\mathfrak{U}_{i+2,j-1}^{k+1}+\mathfrak{U}_{i+2,j-1}^{k}+\mathfrak{U}_{i,j+1}^{k})+\mathfrak{C}_2(\mathfrak{U}_{i+2,j+1}^{k+1}+\mathfrak{U}_{i,j-1}^{k+1}\\
&+\mathfrak{U}_{i+2,j+1}^{k}+\mathfrak{U}_{i,j-1}^{k})+(\mathfrak{N}^{i+1,j,k}-\sigma^{i+1,j,k}\mathcal{W}_{1}^{i+1,j,k}-2\mathfrak{C}_1\\
&-2\mathfrak{C}_2)\mathfrak{U}_{i+1,j}^{k}+\sigma^{i+1,j,k}\sum_{s=1}^{k-1}\left(\mathcal{W}_{k-s}^{i+1,j,k}-\mathcal{W}_{k-s+1}^{i+1,j,k}\right)\mathfrak{U}_{i+1,j}^{s}\\
&+\sigma^{i+1,j,k}\mathcal{W}_{k}^{i+1,j,k}\mathfrak{U}_{i+1,j}^{0}+f_{i+1,j}^{k+1/2},\\
rhs_{i,j+1}=&\mathfrak{C}_1(\mathfrak{U}_{i-1,j+2}^{k+1}+\mathfrak{U}_{i+1,j}^{k}+\mathfrak{U}_{i-1,j+2}^{k})+\mathfrak{C}_2(\mathfrak{U}_{i+1,j+2}^{k+1}+\mathfrak{U}_{i-1,j}^{k+1}\\
&+\mathfrak{U}_{i+1,j+2}^{k}+\mathfrak{U}_{i-1,j}^{k})+(\mathfrak{N}^{i,j+1,k}-\sigma^{i,j+1,k}\mathcal{W}_{1}^{i,j+1,k}-2\mathfrak{C}_1\\
&-2\mathfrak{C}_2)\mathfrak{U}_{i,j+1}^{k}+\sigma^{i,j+1,k}\sum_{s=1}^{k-1}\left(\mathcal{W}_{k-s}^{i,j+1,k}-\mathcal{W}_{k-s+1}^{i,j+1,k}\right)\mathfrak{U}_{i,j+1}^{s}\\
&+\sigma^{i,j+1,k}\mathcal{W}_{k}^{i,j+1,k}\mathfrak{U}_{i,j+1}^{0}+f_{i,j+1}^{k+1/2}.
\end{aligned}
$$

The last $(4\times4)$ system of equations can be decoupled into two $(2\times2)$ systems whose explicit forms are as follows,

$$
\begin{bmatrix}\mathfrak{U}_{i,j}^{k+1}\\ \mathfrak{U}_{i+1,j+1}^{k+1}\end{bmatrix}=\mathfrak{Q}_1\begin{bmatrix}-\mathfrak{D}_2 & -\mathfrak{C}_2\\ -\mathfrak{C}_2 & -\mathfrak{D}_1\end{bmatrix}\begin{bmatrix}rhs_{i,j}\\ rhs_{i+1,j+1}\end{bmatrix} \tag{3.4}
$$

and

$$
\begin{bmatrix}\mathfrak{U}_{i+1,j}^{k+1}\\ \mathfrak{U}_{i,j+1}^{k+1}\end{bmatrix}=\mathfrak{Q}_2\begin{bmatrix}-\mathfrak{D}_4 & -\mathfrak{C}_1\\ -\mathfrak{C}_1 & -\mathfrak{D}_3\end{bmatrix}\begin{bmatrix}rhs_{i+1,j}\\ rhs_{i,j+1}\end{bmatrix}, \tag{3.5}
$$

where

$$
\mathfrak{Q}_1=\frac{1}{\mathfrak{C}_2^2-\mathfrak{D}_1\mathfrak{D}_2},\ \mathfrak{Q}_2=\frac{1}{\mathfrak{C}_1^2-\mathfrak{D}_3\mathfrak{D}_4}.
$$

Figure 1 sheds the light on the grid shape of the EDG method. From the figure, the grid points of the discretized solution domain are branched into two distinct types, namely, black filled diamonds and white filled diamonds. One can easily verify that the implementation of Eq (3.4) involves only points of type ♦, while the implementation of Eq (3.5) requires only points of type ◊. As a result, the computations of Eqs (3.4) and (3.5) can be performed independently.

By keeping these observations into consideration, the EDG method can be completed in two steps. First, the solution values on one type of points are evaluated iteratively by utilizing either Eq (3.4) or Eq (3.5). Second, after convergence is achieved in the first step, the solution values on the residual grid points are computed directly once using Eq (2.5). In this way, the computational cost is reduced effectively as only half of the grid points are involved in the iterative process, which ultimately reduces the execution time of the whole computation process. The application of the EDG method for solving the VO-TFDE will result in a linear system of algebraic equations. Following a similar manner in section two, it can be easily verified that the coefficient matrix is a strictly diagonally dominant matrix and, hence, the resulting system is uniquely solvable.

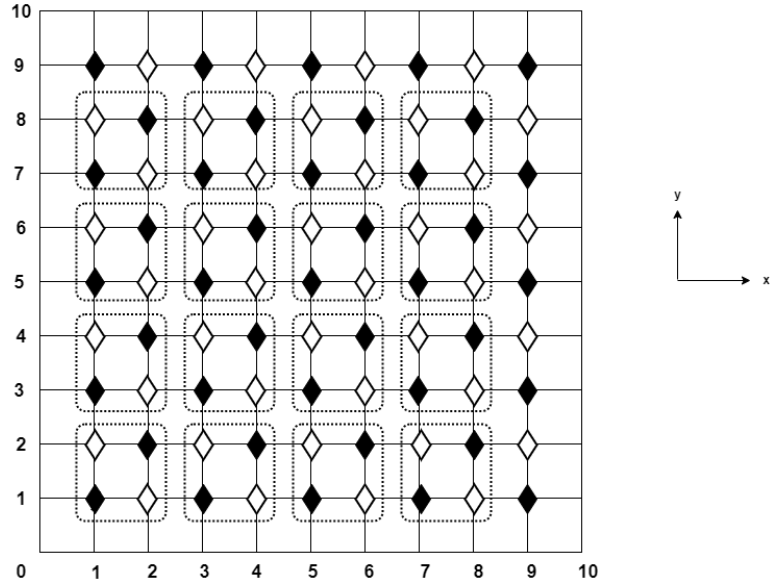


**Figure 1.** Computational molecule for the EDG method with $M_1 = M_2 = 10$.

## 4. Stability analysis

In this section, we analyze the stability of the proposed finite difference approximations via the von-Neumann method. The stability of numerical schemes is one of the most important issues in the realm of numerical analysis that must be addressed. We start by introducing the following lemma that will be utilized in the stability analysis,

**Lemma 1.** *The coefficients* $\mathcal{W}_s^{i,j,k}$, $0 \le i \le M_1 - 1$, $0 \le j \le M_2 - 1$ *defined in Eqs (2.5) and (3.2) satisfy the following properties [61],*

(i) $\mathcal{W}_s^{i,j,k} \ge \mathcal{W}_{s+1}^{i,j,k}$, $1 \le s \le k = 1, 2, \ldots, N-1$.
(ii) $\sum_{s=1}^{k-1} \left( \mathcal{W}_{k-s}^{i,j,k} - \mathcal{W}_{k-s+1}^{i,j,k} \right) = \mathcal{W}_1^{i,j,k} - \mathcal{W}_k^{i,j,k}$.

Let $\hat{\mathfrak{U}}_{i,j}^k$ and $\bar{\mathfrak{U}}_{i,j}^k$ represent the numerical solutions of Eqs (2.5) and (3.2), respectively, then the errors can be defined as:

$$\xi_{i,j}^k = \mathfrak{U}_{i,j}^k - \hat{\mathfrak{U}}_{i,j}^k, \ 0 \le i \le M_1, \ 0 \le j \le M_2, \ 1 \le k \le N, \tag{4.1}$$

$$\varepsilon_{i,j}^k = \mathfrak{U}_{i,j}^k - \bar{\mathfrak{U}}_{i,j}^k, \ 0 \le i \le M_1, \ 0 \le j \le M_2, \ 1 \le k \le N. \tag{4.2}$$

Next, by setting (4.1) into (2.5), we obtain

$$\begin{aligned} &(\mathfrak{A}^{i,j,k} + 2\mathfrak{B}_1 + 2\mathfrak{B}_2)\xi_{i,j}^{k+1} - \mathfrak{B}_1(\xi_{i+1,j}^{k+1} + \xi_{i-1,j}^{k+1}) - \mathfrak{B}_2(\xi_{i,j+1}^{k+1} + \xi_{i,j-1}^{k+1}) = \\ &\mathfrak{B}_1(\xi_{i+1,j}^{k} + \xi_{i-1,j}^{k}) + \mathfrak{B}_2(\xi_{i,j+1}^{k} + \xi_{i,j-1}^{k}) + (\mathfrak{A}^{i,j,k} - \sigma^{i,j,k}\mathcal{W}_1^{i,j,k} - 2\mathfrak{B}_1 - 2\mathfrak{B}_2)\xi_{i,j}^{k} \\ &+ \sigma^{i,j,k} \sum_{s=1}^{k-1} \left( \mathcal{W}_{k-s}^{i,j,k} - \mathcal{W}_{k-s+1}^{i,j,k} \right) \xi_{i,j}^{s} + \sigma^{i,j,k}\mathcal{W}_k^{i,j,k}\xi_{i,j}^{0}. \end{aligned} \tag{4.3}$$

Similarly, replacing (4.2) into (3.2), we have

$$\begin{aligned}&(\mathfrak{A}^{i,j,k}+2\mathfrak{C}_1+2\mathfrak{C}_2)\varepsilon_{i,j}^{k+1}-\mathfrak{C}_1(\varepsilon_{i+1,j-1}^{k+1}+\varepsilon_{i-1,j+1}^{k+1})-\mathfrak{C}_2(\varepsilon_{i+1,j+1}^{k+1}+\varepsilon_{i-1,j-1}^{k+1})=\\&\mathfrak{C}_1(\varepsilon_{i+1,j-1}^{k}+\varepsilon_{i-1,j+1}^{k})+\mathfrak{C}_2(\varepsilon_{i+1,j+1}^{k}+\varepsilon_{i-1,j-1}^{k})+(\mathfrak{A}^{i,j,k}-\sigma^{i,j,k}W_1^{i,j,k}-2\mathfrak{C}_1-2\mathfrak{C}_2)\varepsilon_{i,j}^{k}\\&+\sigma^{i,j,k}\sum_{s=1}^{k-1}\left(\mathcal{W}_{k-s}^{i,j,k}-\mathcal{W}_{k-s+1}^{i,j,k}\right)\varepsilon_{i,j}^{s}+\sigma^{i,j,k}\mathcal{W}_{k}^{i,j,k}\varepsilon_{i,j}^{0}.\end{aligned}\tag{4.4}$$

Then, $\xi^k(x,y)$ and $\varepsilon^k(x,y)$ can be expanded in the Fourier series as

$$\begin{aligned}\xi^k(x,y)&=\sum_{Z_1=-\infty}^{\infty}\sum_{Z_2=-\infty}^{\infty}\eta^k(Z_1,Z_2)e^{2\pi I(Z_1x/L+Z_2y/L)},\\\varepsilon^k(x,y)&=\sum_{Z_1=-\infty}^{\infty}\sum_{Z_2=-\infty}^{\infty}\mu^k(Z_1,Z_2)e^{2\pi I(Z_1x/L+Z_2y/L)},\end{aligned}\tag{4.5}$$

where $I=\sqrt{-1}$ and $\eta^k$ and $\mu^k$ are given by

$$\eta^k(Z_1,Z_2)=\frac{1}{L^2}\int_0^L\int_0^L\xi^k(x,y)e^{-2\pi I(Z_1x/L+Z_2y/L)}dxdy,\tag{4.6}$$

$$\mu^k(Z_1,Z_2)=\frac{1}{L^2}\int_0^L\int_0^L\varepsilon^k(x,y)e^{-2\pi I(Z_1x/L+Z_2y/L)}dxdy.\tag{4.7}$$

Based on the definition of $l^2$ norm and the Pareval equality, we obtain

$$\begin{aligned}\|\xi^k\|_2&=\left(\sum_{Z_2=-\infty}^{\infty}\sum_{Z_1=-\infty}^{\infty}|\eta^k(Z_1,Z_2)|^2\right)^{1/2},\\\|\varepsilon^k\|_2&=\left(\sum_{Z_2=-\infty}^{\infty}\sum_{Z_1=-\infty}^{\infty}|\mu^k(Z_1,Z_2)|^2\right)^{1/2}.\end{aligned}\tag{4.8}$$

Suppose that the solutions of Eqs (4.3) and (4.4) can be written as

$$\xi_{i,j}^k=\eta^k e^{I(\gamma_1 i\Delta x+\gamma_2 j\Delta y)},\quad \varepsilon_{i,j}^k=\mu^k e^{I(\gamma_1 i\Delta x+\gamma_2 j\Delta y)},\tag{4.9}$$

in which $\gamma_1=2\pi Z_1/L$ and $\gamma_2=2\pi Z_2/L$.
Substituting $\xi_{i,j}^k=\eta^k e^{I(\gamma_1 i\Delta x+\gamma_2 j\Delta y)}$ into Eq (16), we get

$$\begin{aligned}\eta^{k+1}=&\frac{\mathfrak{A}^{i,j,k}-\rho_1-\rho_2-\sigma^{i,j,k}\mathcal{W}_1^{i,j,k}}{\mathfrak{A}^{i,j,k}+\rho_1+\rho_2}\eta^k\\&+\frac{1}{\mathfrak{A}^{i,j,k}+\rho_1+\rho_2}\left[\sigma^{i,j,k}\sum_{s=1}^{k-1}\left(\mathcal{W}_{k-s}^{i,j,k}-\mathcal{W}_{k-s+1}^{i,j,k}\right)\eta^s+\sigma^{i,j,k}\mathcal{W}_{k}^{i,j,k}\eta^0\right],\end{aligned}\tag{4.10}$$

where

$$\rho_1=4\mathfrak{B}_1\sin^2\left(\frac{\gamma_1\Delta x}{2}\right),\ \rho_2=4\mathfrak{B}_2\sin^2\left(\frac{\gamma_2\Delta y}{2}\right).$$

Next, we prove the following result.

**Lemma 2.** *If $\eta^k$ $(1 \le k \le N)$ satisfies Eq (4.10) and $2 \ge 3^{1-\alpha^{i,j,k}}$, then, $|\eta^k| \le |\eta^0|$.*

*Proof.* We utilize mathematical induction to complete the proof. First, let $k = 0$, and we get

$$\left|\eta^1\right| = \left|\frac{\mathfrak{A}^{i,j,k} - \rho_1 - \rho_2}{\mathfrak{A}^{i,j,k} + \rho_1 + \rho_2}\right|\left|\eta^0\right|.$$

Since $\mathfrak{A}^{i,j,k}$, $\rho_1$ and $\rho_2$ are nonnegative numbers, then,

$$\left|\eta^1\right| \le \left|\eta^0\right|.$$

Now, suppose that $\left|\eta^{m+1}\right| \le \left|\eta^0\right|$, $m = 0, 1, 2, \ldots, k-1$.We show it holds for $m = k$. Using Eq (4.10) and Lemma 1, we get

$$\begin{aligned}
\left|\eta^{k+1}\right| \le & \left|\frac{\mathfrak{A}^{i,j,k} - \rho_1 - \rho_2 - \sigma^{i,j,k}\mathcal{W}_1^{i,j,k}}{\mathfrak{A}^{i,j,k} + \rho_1 + \rho_2}\right|\left|\eta^k\right| \\
& + \left|\frac{1}{\mathfrak{A}^{i,j,k} + \rho_1 + \rho_2}\right|\left[\sigma^{i,j,k}\sum_{s=1}^{k-1}\left(\mathcal{W}_{k-s}^{i,j,k} - \mathcal{W}_{k-s+1}^{i,j,k}\right)|\eta^s| + \sigma^{i,j,k}\mathcal{W}_k^{i,j,k}\left|\eta^0\right|\right] \\
& \le \left|\frac{\mathfrak{A}^{i,j,k} - \rho_1 - \rho_2 - \sigma^{i,j,k}\mathcal{W}_1^{i,j,k}}{\mathfrak{A}^{i,j,k} + \rho_1 + \rho_2}\right|\left|\eta^0\right| \\
& + \frac{1}{\mathfrak{A}^{i,j,k} + \rho_1 + \rho_2}\left[\sigma^{i,j,k}\sum_{s=1}^{k-1}\left(\mathcal{W}_{k-s}^{i,j,k} - \mathcal{W}_{k-s+1}^{i,j,k}\right)\left|\eta^0\right| + \sigma^{i,j,k}\mathcal{W}_k^{i,j,k}\left|\eta^0\right|\right] \\
& = \frac{\left|\mathfrak{A}^{i,j,k} - \rho_1 - \rho_2 - \sigma^{i,j,k}\mathcal{W}_1^{i,j,k}\right| + \sigma^{i,j,k}\mathcal{W}_1^{i,j,k}}{\mathfrak{A}^{i,j,k} + \rho_1 + \rho_2}\left|\eta^0\right|.
\end{aligned}$$

If $\mathfrak{A}^{i,j,k} - \rho_1 - \rho_2 - \sigma^{i,j,k}\mathcal{W}_1^{i,j,k} > 0$, then

$$\left|\eta^{k+1}\right| \le \frac{\mathfrak{A}^{i,j,k} - \rho_1 - \rho_2}{\mathfrak{A}^{i,j,k} + \rho_1 + \rho_2}\left|\eta^0\right| < \left|\eta^0\right|.$$

If $\mathfrak{A}^{i,j,k} - \rho_1 - \rho_2 - \sigma^{i,j,k}\mathcal{W}_1^{i,j,k} < 0$, then

$$\left|\eta^{k+1}\right| \le \frac{-\mathfrak{A}^{i,j,k} + \rho_1 + \rho_2 + 2\sigma^{i,j,k}\mathcal{W}_1^{i,j,k}}{\mathfrak{A}^{i,j,k} + \rho_1 + \rho_2}\left|\eta^0\right|.$$

Here,

$$\begin{aligned}
\left|\eta^{k+1}\right| \le \left|\eta^0\right| & \\
& \Leftrightarrow \frac{-\mathfrak{A}^{i,j,k} + \rho_1 + \rho_2 + 2\sigma^{i,j,k}\mathcal{W}_1^{i,j,k}}{\mathfrak{A}^{i,j,k} + \rho_1 + \rho_2} \le 1 \\
& \Leftrightarrow -\mathfrak{A}^{i,j,k} + \rho_1 + \rho_2 + 2\sigma^{i,j,k}\mathcal{W}_1^{i,j,k} \le \mathfrak{A}^{i,j,k} + \rho_1 + \rho_2 \\
& \Leftrightarrow 2 \ge 3^{1-\alpha^{i,j,k}}.
\end{aligned}$$

□

Now, we prove the next theorem.

**Theorem 1.** *If* $2 \geq 3^{1-\alpha^{i,j,k}}$*, then the finite difference scheme defined by Eq (2.5) is stable.*

*Proof.* From Lemma 2 and the Parseval equality, we have

$$\|\xi^k\|_2^2 = \sum_{Z_1=-\infty}^{\infty} \sum_{Z_2=-\infty}^{\infty} \left|\eta^k(Z_1, Z_2)\right|^2 \leq \sum_{Z_1=-\infty}^{\infty} \sum_{Z_2=-\infty}^{\infty} \left|\eta^0(Z_1, Z_2)\right|^2 = \|\xi^0\|_2^2,$$

from which we get,

$$\|\xi^k\| \leq \|\xi^0\|.$$

□

Setting $\varepsilon_{i,j}^k = \mu^k e^{I(\gamma_1 i\Delta x + \gamma_2 j\Delta y)}$ into Eq (4.4) gives

$$\begin{aligned}\mu^{k+1} =& \frac{\mathfrak{V}^{i,j,k} - \kappa_1 - \kappa_2 - \sigma^{i,j,k}\mathcal{W}_1^{i,j,k}}{\mathfrak{V}^{i,j,k} + \kappa_1 + \kappa_2}\mu^k \\ &+ \frac{1}{\mathfrak{V}^{i,j,k} + \kappa_1 + \kappa_2}\left[\sigma^{i,j,k}\sum_{s=1}^{k-1}\left(\mathcal{W}_{k-s}^{i,j,k} - \mathcal{W}_{k-s+1}^{i,j,k}\right)\mu^s + \sigma^{i,j,k}\mathcal{W}_k^{i,j,k}\mu^0\right],\end{aligned} \tag{4.11}$$

in which

$$\kappa_1 = 4\mathfrak{C}_1 \sin^2\left(\frac{\gamma_1\Delta x - \gamma_2\Delta y}{2}\right),\ \kappa_2 = 4\mathfrak{C}_2 \sin^2\left(\frac{\gamma_1\Delta x + \gamma_2\Delta y}{2}\right).$$

**Lemma 3.** *If* $\mu^k$ $(1 \leq k \leq N)$ *satisfies Eq (4.11) and* $2 \geq 3^{1-\alpha^{i,j,k}}$*, then,* $|\mu^k| \leq |\mu^0|$.

*Proof.* First, putting $k = 0$ in Eq (4.11), we obtain

$$\left|\mu^1\right| = \left|\frac{\mathfrak{V}^{i,j,k} - \kappa_1 - \kappa_2}{\mathfrak{V}^{i,j,k} + \kappa_1 + \kappa_2}\right|\left|\mu^0\right| < \left|\mu^0\right|.$$

Next, assume that $\left|\mu^{m+1}\right| \leq \left|\mu^0\right|$, $m = 0, 1, 2, \ldots, k-1$. We prove it is true for $m = k$. With the help of Eq (4.11) and Lemma 1, we obtain

$$\begin{aligned}\left|\mu^{k+1}\right| \leq& \left|\frac{\mathfrak{V}^{i,j,k} - \kappa_1 - \kappa_2 - \sigma^{i,j,k}\mathcal{W}_1^{i,j,k}}{\mathfrak{V}^{i,j,k} + \kappa_1 + \kappa_2}\right|\left|\mu^k\right| \\ &+ \left|\frac{1}{\mathfrak{V}^{i,j,k} + \kappa_1 + \kappa_2}\right|\left[\sigma^{i,j,k}\sum_{s=1}^{k-1}\left(\mathcal{W}_{k-s}^{i,j,k} - \mathcal{W}_{k-s+1}^{i,j,k}\right)|\mu^s| + \sigma^{i,j,k}\mathcal{W}_k^{i,j,k}\left|\mu^0\right|\right] \\ &\leq \left|\frac{\mathfrak{V}^{i,j,k} - \kappa_1 - \kappa_2 - \sigma^{i,j,k}\mathcal{W}_1^{i,j,k}}{\mathfrak{V}^{i,j,k} + \kappa_1 + \kappa_2}\right|\left|\mu^0\right| \\ &+ \frac{1}{\mathfrak{V}^{i,j,k} + \kappa_1 + \kappa_2}\left[\sigma^{i,j,k}\sum_{s=1}^{k-1}\left(\mathcal{W}_{k-s}^{i,j,k} - \mathcal{W}_{k-s+1}^{i,j,k}\right)\left|\mu^0\right| + \sigma^{i,j,k}\mathcal{W}_k^{i,j,k}\left|\mu^0\right|\right] \\ &= \frac{\left|\mathfrak{V}^{i,j,k} - \kappa_1 - \kappa_2 - \sigma^{i,j,k}\mathcal{W}_1^{i,j,k}\right| + \sigma^{i,j,k}\mathcal{W}_1^{i,j,k}}{\mathfrak{V}^{i,j,k} + \kappa_1 + \kappa_2}\left|\mu^0\right|.\end{aligned}$$

If $\mathfrak{A}^{i,j,k} - \kappa_1 - \kappa_2 - \sigma^{i,j,k}\mathcal{W}_1^{i,j,k} > 0$, then

$$\left|\mu^{k+1}\right| \leq \frac{\mathfrak{A}^{i,j,k} - \kappa_1 - \kappa_2}{\mathfrak{A}^{i,j,k} + \kappa_1 + \kappa_2}\left|\mu^0\right| < \left|\mu^0\right|.$$

If $\mathfrak{A}^{i,j,k} - \kappa_1 - \kappa_2 - \sigma^{i,j,k}\mathcal{W}_1^{i,j,k} < 0$, then

$$\left|\mu^{k+1}\right| \leq \frac{-\mathfrak{A}^{i,j,k} + \kappa_1 + \kappa_2 + 2\sigma^{i,j,k}\mathcal{W}_1^{i,j,k}}{\mathfrak{A}^{i,j,k} + \kappa_1 + \kappa_2}\left|\mu^0\right|.$$

Here,

$$\begin{aligned}
&\left|\mu^{k+1}\right| \leq \left|\mu^0\right| \\
&\quad \Leftrightarrow \frac{-\mathfrak{A}^{i,j,k} + \kappa_1 + \kappa_2 + 2\sigma^{i,j,k}\mathcal{W}_1^{i,j,k}}{\mathfrak{A}^{i,j,k} + \kappa_1 + \kappa_2} \leq 1 \\
&\quad \Leftrightarrow -\mathfrak{A}^{i,j,k} + \kappa_1 + \kappa_2 + 2\sigma^{i,j,k}\mathcal{W}_1^{i,j,k} \leq \mathfrak{A}^{i,j,k} + \kappa_1 + \kappa_2 \\
&\quad \Leftrightarrow 2 \geq 3^{1-\alpha^{i,j,k}}.
\end{aligned}$$

□

Now, Lemma 2 is employed to prove the next theorem.

**Theorem 2.** *If $2 \geq 3^{1-\alpha^{i,j,k}}$, then, the finite difference scheme defined by Eq (3.2) is stable.*

*Proof.* From Lemma 3 and the Parseval equality, we have

$$\|\varepsilon^k\|_2^2 = \sum_{Z_1=-\infty}^{\infty}\sum_{Z_2=-\infty}^{\infty}\left|\mu^k(Z_1, Z_2)\right|^2 \leq \sum_{Z_1=-\infty}^{\infty}\sum_{Z_2=-\infty}^{\infty}\left|\mu^0(Z_1, Z_2)\right|^2 = \|\varepsilon^0\|_2^2,$$

which gives the desired result

$$\|\varepsilon^k\| \leq \|\varepsilon^0\|.$$

□

## 5. Convergence analysis

This section is devoted to analyze the convergence of the proposed methods. Let $\zeta_{i,j}^k$ be the difference between the exact and numerical solutions at the point $(x_i, y_j, t_k)$, then the error can be written as,

$$\zeta_{i,j}^k = u_{i,j}^k - \mathfrak{U}_{i,j}^k,\ 1 \leq i \leq M_1 - 1,\ 1 \leq j \leq M_2 - 1,\ 1 \leq k \leq N. \tag{5.1}$$

By setting Eq (5.1) into Eq (2.5), the error equation follows immediately as

$$\begin{aligned}
&(\mathfrak{A}^{i,j,k} + 2\mathfrak{B}_1 + 2\mathfrak{B}_2)\zeta_{i,j}^{k+1} - \mathfrak{B}_1(\zeta_{i+1,j}^{k+1} + \zeta_{i-1,j}^{k+1}) - \mathfrak{B}_2(\zeta_{i,j+1}^{k+1} + \zeta_{i,j-1}^{k+1}) = \\
&\mathfrak{B}_1(\zeta_{i+1,j}^{k} + \zeta_{i-1,j}^{k}) + \mathfrak{B}_2(\zeta_{i,j+1}^{k} + \zeta_{i,j-1}^{k}) + (\mathfrak{A}^{i,j,k} - \sigma^{i,j,k}\mathcal{W}_1^{i,j,k} - 2\mathfrak{B}_1 \\
&- 2\mathfrak{B}_2)\zeta_{i,j}^{k} + \sigma^{i,j,k}\sum_{s=1}^{k-1}\left(\mathcal{W}_{k-s}^{i,j,k} - \mathcal{W}_{k-s+1}^{i,j,k}\right)\zeta_{i,j}^{s} + \sigma^{i,j,k}\mathcal{W}_k^{i,j,k}\zeta_{i,j}^{0} + R_{i,j}^{k+1/2},
\end{aligned} \tag{5.2}$$

where $R_{i,j}^{k+1/2}$ denotes the truncation error at the point $(x_i, y_j, t_{k+1/2})$. From now on, we suppose that $C$ is a constant that may take different values at different locations. From Eq (2.4), we have

$$\left|R_{i,j}^{k+1/2}\right| \leq C(\tau + (\Delta x)^2 + (\Delta y)^2),\ 1 \leq i \leq M_1 - 1,\ 1 \leq j \leq M_2 - 1,\ 0 \leq k \leq N, \tag{5.3}$$

where

$$C = \max_{1\leq i\leq M_1-1, 1\leq j\leq M_2-1, 0\leq k\leq N}\{C_{i,j}^k\}.$$

Next, $\zeta^k(x, y)$ and $R^{k+1/2}(x, y)$ can be expanded in the Fourier series as

$$\zeta^k(x, y) = \sum_{Z_2=-\infty}^{\infty}\sum_{Z_1=-\infty}^{\infty} \psi^k(Z_1, Z_2)e^{2\pi I(Z_1 x/L+Z_2 y/L)},$$

$$R^{k+1/2}(x, y) = \sum_{Z_2=-\infty}^{\infty}\sum_{Z_1=-\infty}^{\infty} \phi^k(Z_1, Z_2)e^{2\pi I(Z_1 x/L+Z_2 y/L)},$$

such that

$$\psi^k(Z_1, Z_2) = \frac{1}{L^2}\int_0^L\int_0^L \zeta^k(x, y)e^{-2\pi I(Z_1 x/L+Z_2 y/L)}dxdy,$$

$$\phi^k(Z_1, Z_2) = \frac{1}{L^2}\int_0^L\int_0^L R^{k+1/2}(x, y)e^{-2\pi I(Z_1 x/L+Z_2 y/L)}dxdy.$$

Considering the definition of $l^2$ norm and the Parseval equality, we get

$$\|\zeta^k\|_2 = \left(\sum_{j=1}^{M_2-1}\sum_{i=1}^{M_1-1} \Delta y\Delta x\left|\zeta_{i,j}^k\right|^2\right)^{1/2} = \left(\sum_{Z_1=-\infty}^{\infty}\sum_{Z_2=-\infty}^{\infty} \left|\psi^k(Z_1, Z_2)\right|^2\right)^{1/2}, \tag{5.4}$$

$$\|R^{k+1/2}\|_2 = \left(\sum_{j=1}^{M_2-1}\sum_{i=1}^{M_1-1} \Delta y\Delta x\left|R_{i,j}^{k+1/2}\right|^2\right)^{1/2} = \left(\sum_{Z_1=-\infty}^{\infty}\sum_{Z_2=-\infty}^{\infty} \left|\phi^k(Z_1, Z_2)\right|^2\right)^{1/2}. \tag{5.5}$$

Suppose the solutions of Eq (5.2) are as follows:

$$\zeta_{i,j}^k = \psi^k e^{I(\gamma_1 i\Delta x+\gamma_2 j\Delta y)},\ R_{i,j}^{k+1/2} = \phi^{k+1/2}e^{I(\gamma_1 i\Delta x+\gamma_2 j\Delta y)}. \tag{5.6}$$

Substitute Eq (5.6) into Eq (5.2) and simplify to emerge with the following expression,

$$\begin{aligned}\psi^{k+1} =& \frac{\mathfrak{V}^{i,j,k} - \rho_1 - \rho_2 - \sigma^{i,j,k}\mathcal{W}_1^{i,j,k}}{\mathfrak{V}^{i,j,k} + \rho_1 + \rho_2}\psi^k \\ &+ \frac{1}{\mathfrak{V}^{i,j,k} + \rho_1 + \rho_2}\left[\sigma^{i,j,k}\sum_{s=1}^{k-1}\left(\mathcal{W}_{k-s}^{i,j,k} - \mathcal{W}_{k-s+1}^{i,j,k}\right)\psi^s + \sigma^{i,j,k}\mathcal{W}_k^{i,j,k}\psi^0 + \phi^{k+1/2}\right],\end{aligned} \tag{5.7}$$

where $\rho_1$ and $\rho_2$ are as defined in Eq (4.10).

**Lemma 4.** *If $\psi^k$ $(1 \leq k \leq N)$ satisfies Eq (5.7), then, we have*

$$\left|\psi^{k+1}\right| \leq C(k + 1)\tau\left|\phi^{1/2}\right|.$$

*Proof.* From Eq (5.5), there is a positive constant $C$ such that

$$\left|\phi^{k+1/2}\right| \le C\tau\left|\phi^{1/2}\right|,\ 0 \le k \le N-1.$$

We complete the proof by mathematical induction. First, setting $k = 0$ in Eq (5.7) and noticing that $\psi^0 = 0$, we obtain

$$\left|\psi^1\right| = \frac{1}{\mathfrak{A}^{i,j,k} + \rho_1 + \rho_2}\left|\phi^{1/2}\right| \le \left|\phi^{1/2}\right| \le C\tau\left|\phi^{1/2}\right|.$$

Next, assume that

$$\left|\psi^{m+1}\right| \le C(m+1)\tau\left|\phi^{1/2}\right|,\ m = 0, 1, 2, \ldots, k-1.$$

Putting $m = k$ in Eq (5.7) and using Lemma 1, we get

$$\begin{aligned}
\left|\psi^{k+1}\right| \le & \left|\frac{\mathfrak{A}^{i,j,k} - \rho_1 - \rho_2 - \sigma^{i,j,k}\mathcal{W}_1^{i,j,k}}{\mathfrak{A}^{i,j,k} + \rho_1 + \rho_2}\right|\left|\psi^k\right| \\
& + \left|\frac{1}{\mathfrak{A}^{i,j,k} + \rho_1 + \rho_2}\right|\left[\sigma^{i,j,k}\sum_{s=1}^{k-1}\left(\mathcal{W}_{k-s}^{i,j,k} - \mathcal{W}_{k-s+1}^{i,j,k}\right)|\psi^s| + \sigma^{i,j,k}\mathcal{W}_k^{i,j,k}\left|\psi^0\right| + \left|\phi^{k+1/2}\right|\right] \\
& \le \frac{\left|\mathfrak{A}^{i,j,k} - \rho_1 - \rho_2 - \sigma^{i,j,k}\mathcal{W}_1^{i,j,k}\right|}{\mathfrak{A}^{i,j,k} + \rho_1 + \rho_2}Ck\tau\left|\phi^{1/2}\right| \\
& + \frac{1}{\mathfrak{A}^{i,j,k} + \rho_1 + \rho_2}\left[\sigma^{i,j,k}Ck\tau\left|\phi^{1/2}\right|\left(\sum_{s=1}^{k-1}\left(\mathcal{W}_{k-s}^{i,j,k} - \mathcal{W}_{k-s+1}^{i,j,k}\right) + \mathcal{W}_k^{i,j,k}\right) + C\tau\left|\phi^{1/2}\right|\right] \\
& = \frac{\left|\mathfrak{A}^{i,j,k} - \rho_1 - \rho_2 - \sigma^{i,j,k}\mathcal{W}_1^{i,j,k}\right| + \sigma^{i,j,k}\mathcal{W}_1^{i,j,k}}{\mathfrak{A}^{i,j,k} + \rho_1 + \rho_2}Ck\tau\left|\phi^{1/2}\right| \\
& + \frac{1}{\mathfrak{A}^{i,j,k} + \rho_1 + \rho_2}C\tau\left|\phi^{1/2}\right| \\
& = \left[\frac{\left|\mathfrak{A}^{i,j,k} - \rho_1 - \rho_2 - \sigma^{i,j,k}\mathcal{W}_1^{i,j,k}\right| + \sigma^{i,j,k}\mathcal{W}_1^{i,j,k}}{\mathfrak{A}^{i,j,k} + \rho_1 + \rho_2}k + \frac{1}{\mathfrak{A}^{i,j,k} + \rho_1 + \rho_2}\right]C\tau\left|\phi^{1/2}\right|.
\end{aligned}$$

If $\mathfrak{A}^{i,j,k} - \rho_1 - \rho_2 - \sigma^{i,j,k}\mathcal{W}_1^{i,j,k} > 0$, then

$$\begin{aligned}
\left|\psi^{k+1}\right| &\le \left[\frac{\mathfrak{A}^{i,j,k} - \rho_1 - \rho_2}{\mathfrak{A}^{i,j,k} + \rho_1 + \rho_2}k + \frac{1}{\mathfrak{A}^{i,j,k} + \rho_1 + \rho_2}\right]C\tau\left|\phi^{1/2}\right| \\
&\le C(k+1)\tau\left|\phi^{1/2}\right|.
\end{aligned}$$

If $\mathfrak{A}^{i,j,k} - \rho_1 - \rho_2 - \sigma^{i,j,k}\mathcal{W}_1^{i,j,k} < 0$, then

$$\left|\psi^{k+1}\right| \le \left[\frac{-\mathfrak{A}^{i,j,k} + \rho_1 + \rho_2 + 2\sigma^{i,j,k}\mathcal{W}_1^{i,j,k}}{\mathfrak{A}^{i,j,k} + \rho_1 + \rho_2}k + \frac{1}{\mathfrak{A}^{i,j,k} + \rho_1 + \rho_2}\right]C\tau\left|\phi^{1/2}\right|.$$

Here,

$$\left|\psi^{k+1}\right| \le C(k+1)\tau\left|\phi^{1/2}\right|$$

$$\Leftrightarrow \frac{-\mathfrak{A}^{i,j,k} + \rho_1 + \rho_2 + 2\sigma^{i,j,k}\mathcal{W}_1^{i,j,k}}{\mathfrak{A}^{i,j,k} + \rho_1 + \rho_2} \leq 1$$
$$\Leftrightarrow -\mathfrak{A}^{i,j,k} + \rho_1 + \rho_2 + 2\sigma^{i,j,k}\mathcal{W}_1^{i,j,k} \leq \mathfrak{A}^{i,j,k} + \rho_1 + \rho_2$$
$$\Leftrightarrow 2 \geq 3^{1-\alpha^{i,j,k}}.$$

Therefore, under the above condition we have

$$\left|\psi^{k+1}\right| \leq C(k+1)\tau\left|\phi^{1/2}\right|.$$

□

We utilize Lemma 4 to prove the next result.

**Theorem 3.** *If* $2 \geq 3^{1-\alpha^{i,j,k}}$*, then the finite difference scheme defined by Eq (2.5) is* $l^2$ *convergent with convergence order* $O(\tau + (\Delta x)^2 + (\Delta y)^2)$.

*Proof.* With the help of Lemma 4 and Eqs (5.4) and (5.5), we obtain

$$\|\zeta^k\|_2^2 = \sum_{Z_1=-\infty}^{\infty}\sum_{Z_2=-\infty}^{\infty}\left|\psi^k(Z_1,Z_2)\right|^2 \leq \sum_{Z_1=-\infty}^{\infty}\sum_{Z_2=-\infty}^{\infty} C^2(k+1)^2\tau^2\left|\phi^{1/2}(Z_1,Z_2)\right|^2$$
$$= C^2(k+1)^2\tau^2\|R^{1/2}\|_2^2.$$

Taking Eq (5.3) into consideration leads to

$$\|\zeta^k\|_2 \leq C(k+1)\tau\|R^{1/2}\|_2 \leq C(k+1)\tau(\tau + (\Delta x)^2 + (\Delta y)^2)$$
$$\leq C^*(\tau + (\Delta x)^2 + (\Delta y)^2),$$

where $C^* = CT$ as $(k+1)\tau \leq T$. □

**Theorem 4.** *If* $2 \geq 3^{1-\alpha^{i,j,k}}$*, then the finite difference scheme defined by Eq (3.2) is* $l^2$ *convergent with convergence order* $O(\tau + (\Delta x)^2 + (\Delta y)^2)$.

*Proof.* The proof can be established in analogous way to Theorem 3. □

Theorems 3 and 4 indicate the convergence of the numerical schemes (2.5) and (3.2), respectively. This means that as the spatial and temporal step sizes approach zero, the numerical solutions approach to the exact solution of the considered problem. These considerations will be verified in the next section.

## 6. Numerical experiments and discussion of results

### *6.1. Numerical experiments*

After the construction and analysis of the C-N and EDG solution methods in the previous sections, we turn our attention to simulating the two-dimensional VO-TFDE (1.1) using the aforementioned numerical schemes. In this endeavor, three numerical examples are chosen to illustrate the capability, accuracy and efficiency of the presented methods. The exact analytical solution of each example

is known and is utilized for comparison with the evaluated numerical solutions. Unless otherwise specified, the solution domain is set to be $[0,1] \times [0,1] \times (0,1]$. Furthermore, we assume that $\Delta x = \Delta y = h$ throughout numerical experiments. All computations are carried out using the Julia Programming Language and run on a PC with the configuration: Intel(R) Core(TM) i7-8550U CPU 2.00 GHz 8 GB RAM and the Windows 10 (64-bit) operating system. Matlab is also employed for generating some figures. The computational cost and the accuracy of the proposed methods will be reported based on the criteria of CPU time (in seconds) and the maximum absolute error ($MAE$), respectively. The numerical outcomes of these criteria are attained for different values of mesh sizes and various VO functions. Finally, we include some graphical representations to facilitate the discussion of our results.

The $MAE$ between the exact solution and the numerical solution is given by

$$MAE = \max_{1\le i\le M_1-1, 1\le j\le M_2-1, 1\le k\le N} u(x_i, y_j, t_k) - \mathfrak{U}_{i,j}^k.$$

To compute the convergence order ($CO$), we use

$$CO = \frac{\ln\left(MAE(\tau, h_1)/MAE(\tau, h_2)\right)}{\ln\left(h_1/h_2\right)}.$$

**Example 1.** *Consider the following two-dimensional VO-TFDE:*

$$\begin{aligned} {}_0^C D_t^{\alpha(x,y,t)} u(x,y,t) =& \frac{\partial^2 u(x,y,t)}{\partial x^2} + \frac{\partial^2 u(x,y,t)}{\partial y^2} + \frac{6t^{3-a(x,y,t)}}{\Gamma(4-a(x,y,t))}(1-x^2)^2(1-y^2)^2 \\ & - 4t^3((1-y^2)^2(3x^2-1) + (1-x^2)^2(3y^2-1)) \end{aligned}$$

with the initial and boundary conditions

$$\begin{aligned} & u(x,y,0) = 0, \\ & u(x,0,t) = t^3(1-x^2)^2, \quad u(x,1,t) = t^3(1-x^2)^2, \\ & u(0,y,t) = t^3(1-y^2)^2, \quad u(1,y,t) = t^3(1-y^2)^2, \end{aligned}$$

and the exact analytical solution is given by

$$u(x,y,t) = t^3(1-x^2)^2(1-y^2)^2.$$

Tables 1 gives the CPU times and the numerical errors of the proposed methods for a variety of mesh sizes (1/6, 1/12, 1/18, 1/24) with fixed $\tau = 0.01$ and various values of $\alpha(x,y,t)$. In view of this table, it can be seen that the C-N and EDG methods produce accurate results in solving Example 1. Furthermore, as the mesh size increases, the observed maximum errors for all chosen VO derivatives $\alpha(x,y,t)$ decrease. Figure 2 sketches the CPU time of the C-N and EDG methods according to different sizes of space steps with $\alpha(x,y,t) = \frac{10-(xyt)^3}{80}$ and $\alpha(x,y,t) = \frac{9-x^5+t^3}{120}$. We can see that the EDG method significantly outperforms the C-N method in terms of CPU timing. The time reduction percentage of the EDG method compared to the C-N method is (52.74-79.44)%. For instance, Table 1 shows that we need to take $h = 1/24$ in order to obtain the maximum error of 2.4740E-4 using the C-N

method with $\alpha(x, y, t) = \frac{10-(xyt)^3}{80}$, which costs 44.8959 seconds. On the other hand, the EDG method with $h = 1/24$ achieves a maximum error of 3.4746E-4 and the corresponding computing time is only 11.4655 seconds. These results and comparisons justify our effort to establish the EDG method. Figure 3 shows a comparison of the numerical solutions of the proposed methods and the exact solution of Example 1 for $h = 1/24$, $\tau = 0.01$, $x = 0.5$, $\alpha(x, y, t) = \frac{11-\cos(xt)^2}{11}$ and $T = 0.25, 0.5, 0.75, 1$. One can observe from this figure that the behavior of the numerical solutions is the same as that of the exact solution. Figure 4 displays 3D surface plots of the numerical solutions and the maximum errors for the C-N and EDG methods at $h = 1/24$, $\tau = 0.01$ and $\alpha(x, y, t) = \frac{15+\sin(yt)^5}{16}$. It follows that the numerical solutions of the C-N and EDG methods are in good agreement with the exact solutions, which illustrate the accuracy and effectiveness of the proposed methods.

**Table 1.** The CPU times and maximum errors for Example 1 at $T = 1$, $\tau = 0.01$.

| | | C-N method | | EDG method | |
|---|---|---|---|---|---|
| $\alpha(x, y, t)$ | $h$ | CPU time | *MAE* | CPU time | *MAE* |
| $\frac{10-(xyt)^3}{80}$ | 1/6 | 0.2499 | 4.1038E-03 | 0.0937 | 7.0379E-03 |
| | 1/12 | 3.7891 | 1.0223E-03 | 0.8840 | 1.6246E-03 |
| | 1/18 | 16.3650 | 3.3934E-04 | 4.0260 | 6.7900E-04 |
| | 1/24 | 44.8959 | 2.4740E-04 | 11.4655 | 3.4746E-04 |
| $5^{yt-3}$ | 1/6 | 0.4966 | 4.1265E-03 | 0.1284 | 7.0739E-03 |
| | 1/12 | 4.9944 | 1.0522E-03 | 1.2802 | 1.6364E-03 |
| | 1/18 | 18.8372 | 3.6115E-04 | 5.0190 | 6.8719E-04 |
| | 1/ 24 | 51.9460 | 2.5265E-04 | 13.7734 | 3.4547E-04 |
| $\frac{11-\cos(xt)^2}{11}$ | 1/6 | 0.1588 | 3.7833E-03 | 0.0630 | 6.5721E-03 |
| | 1/12 | 1.7410 | 9.5964E-04 | 0.4935 | 1.5089E-03 |
| | 1/18 | 5.9911 | 3.3693E-04 | 1.6087 | 6.3153E-04 |
| | 1/24 | 17.5482 | 1.8718E-04 | 4.5734 | 3.0326E-04 |
| $\frac{15+\sin(yt)^5}{16}$ | 1/6 | 0.2364 | 3.7776E-03 | 0.1117 | 6.5633E-03 |
| | 1/12 | 2.5489 | 9.5797E-04 | 0.8056 | 1.5115E-03 |
| | 1/18 | 12.0167 | 3.3706E-04 | 3.0428 | 6.4030E-04 |
| | 1/24 | 39.0032 | 1.8076E-04 | 8.0181 | 3.0591E-04 |
| $\frac{9-x^5+t^3}{120}$ | 1/6 | 0.3455 | 4.1132E-03 | 0.0837 | 7.0528E-03 |
| | 1/12 | 3.6123 | 1.0282E-03 | 1.1557 | 1.6213E-03 |
| | 1/18 | 15.4070 | 3.5013E-04 | 4.1639 | 7.0226E-04 |
| | 1/24 | 43.8414 | 2.5438E-04 | 13.8434 | 3.3037E-04 |
| $\frac{15-\sin(xyt)^4}{16}$ | 1/6 | 0.3609 | 3.7780E-03 | 0.1149 | 6.5638E-03 |
| | 1/12 | 2.9381 | 9.5677E-04 | 1.0479 | 1.5113E-03 |
| | 1/18 | 11.8527 | 3.3380E-04 | 2.9980 | 6.3989E-04 |
| | 1/24 | 31.7521 | 1.8077E-04 | 8.2564 | 3.0450E-04 |

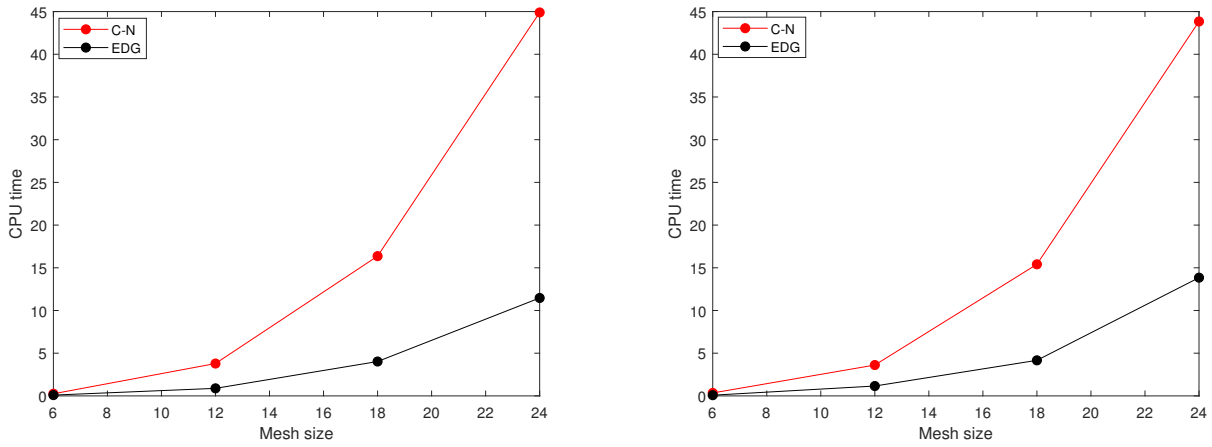


(a) $\alpha(x, y, t) = \frac{10-(xyt)^3}{80}$ (b) $\alpha(x, y, t) = \frac{9-x^5+t^3}{120}$

**Figure 2.** The CPU time comparison of the C-N and EDG methods for Example 1.

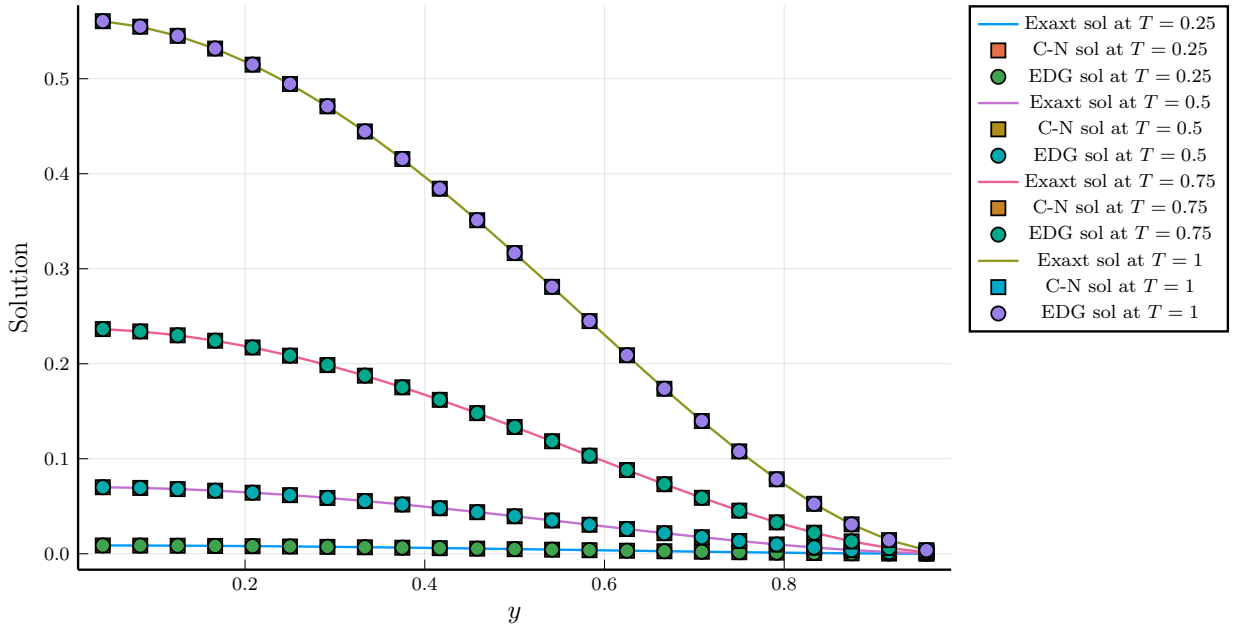


**Figure 3.** Numerical comparison for Example 1 between the exact solution and the numerical solutions obtained using the C-N and EDG methods with $h = 1/24$, $\tau = 0.01$, $x = 0.5$ and $\alpha(x, y, t) = \frac{11-\cos(xt)^2}{11}$.

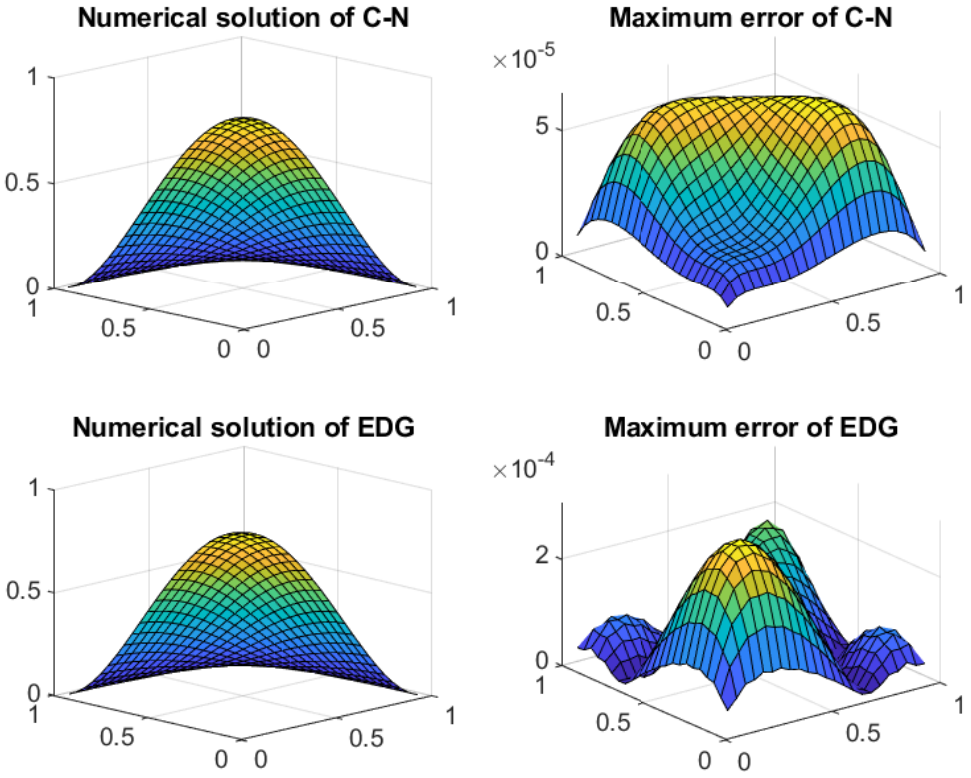


**Figure 4.** The numerical solutions and maximum errors of the C-N and EDG methods with $h = 1/24$, $\tau = 0.01$ and $\alpha(x, y, t) = \frac{15+\sin(yt)^5}{16}$ for Example 1.

**Example 2.** *In this example, we consider the following two-dimensional VO-TFDE:*

$$
\begin{aligned}
{}_0^C D_t^{\alpha(x,y,t)} u(x,y,t) =& \frac{\partial^2 u(x,y,t)}{\partial x^2} + \frac{\partial^2 u(x,y,t)}{\partial y^2} + \frac{2t^{2-a(x,y,t)}}{\Gamma(3-a(x,y,t))} \sin(x^2+y^2) \\
&+ 2t^2(2x^2\sin(x^2+y^2) + 2y^2\sin(x^2+y^2) - 2\cos(x^2+y^2)),
\end{aligned}
$$

subject to the initial and boundary conditions

$$
\begin{aligned}
&u(x,y,0) = 0, \\
&u(x,0,t) = t^2\sin(x^2), \quad u(x,1,t) = t^2\sin(x^2+1), \\
&u(0,y,t) = t^2\sin(y^2), \quad u(1,y,t) = t^2\sin(y^2+1),
\end{aligned}
$$

with the exact analytical solution written as

$$u(x,y,t) = t^2\sin(x^2+y^2).$$

We now utilize the C-N and EDG methods to solve the given problem in Example 2. The CPU times and the maximum errors for several mesh sizes (1/4, 1/10, 1/16, 1/22) with fixed $\tau = 0.01$ and various

values of $\alpha(x, y, t)$ are shown in Table 2. Figure 5 depicts the CPU times of the proposed methods against different values of spatial step sizes for $\alpha(x, y, t) = \frac{e^{xyt}+\cos(xyt)}{30}$ and $\alpha(x, y, t) = \frac{5+(xy)^3-(xt)^4}{50}$. From the data in these tables and figures, it's seen that the C-N and EDG methods generate comparable results in terms of accuracy, but the latter method results in better simulations in terms of CPU timing. From Table 2, the improvement percentage in CPU time of the EDG method compared to the C-N method is (40.36-83.56)%. This example clearly lends itself to a comparison similar to that of Example 1. The numerical solutions of the proposed methods along with the exact solution of Example 2 is portrayed in Figure 6 for $h = 1/22$, $\tau = 0.01$, $x = 0.5$, $\alpha(x, y, t) = \frac{16-e^{xyt}}{17}$ and $T = 0.25, 0.5, 0.75, 1$. Figure 7 highlights the 3D surface plots of the numerical solutions and the maximum errors of the C-N and EDG methods at $h = 1/22$, $\tau = 0.01$ and $\alpha(x, y, t) = \frac{3+(xy)^2-(xt)^3}{30}$. These figures demonstrate the effectiveness of the proposed methods as the numerical solutions are found to match well with the exact analytical solution.

**Table 2.** The CPU times and maximum errors for Example 2 at $T = 1$, $\tau = 0.01$.

| | | C-N method | | EDG method | |
|---|---|---|---|---|---|
| $\alpha(x, y, t)$ | $h$ | CPU time | *MAE* | CPU time | *MAE* |
| $\frac{1-(xyt)^3+\cos(xyt)^2}{10}$ | 1/4 | 0.0876 | 1.0398E-02 | 0.0409 | 2.2604E-02 |
| | 1/10 | 3.2858 | 1.7702E-03 | 0.8188 | 3.3201E-03 |
| | 1/16 | 18.4236 | 7.9260E-04 | 4.9788 | 1.3317E-03 |
| | 1/22 | 63.9827 | 5.9961E-04 | 13.8950 | 7.6442E-04 |
| $\frac{e^{xyt}+\cos(xyt)}{30}$ | 1/4 | 0.2551 | 1.0465E-02 | 0.0497 | 2.2765E-02 |
| | 1/10 | 5.3375 | 1.7854E-03 | 1.2344 | 3.3386E-03 |
| | 1/16 | 25.7313 | 8.1088E-04 | 6.0432 | 1.3401E-03 |
| | 1/22 | 72.5582 | 6.1617E-04 | 22.3957 | 7.9394E-04 |
| $\frac{16-e^{xyt}}{17}$ | 1/4 | 0.0493 | 1.0000E-02 | 0.0294 | 2.1580E-02 |
| | 1/10 | 0.9723 | 1.7134E-03 | 0.3137 | 3.1995E-03 |
| | 1/16 | 5.8175 | 7.8225E-04 | 1.4358 | 1.2959E-03 |
| | 1/22 | 17.8491 | 5.7985E-04 | 4.3844 | 7.4330E-04 |
| $\frac{3+(xy)^2-(xt)^3}{30}$ | 1/4 | 0.0642 | 1.0449E-02 | 0.0227 | 2.2735E-02 |
| | 1/10 | 2.3931 | 1.7715E-03 | 0.8921 | 3.3315E-03 |
| | 1/16 | 14.1170 | 8.2971E-04 | 2.8375 | 1.3347E-03 |
| | 1/22 | 55.0142 | 6.1130E-04 | 9.0424 | 7.7265E-04 |
| $\frac{5+(xy)^3-(xt)^4}{50}$ | 1/4 | 0.0682 | 1.0448E-02 | 0.0291 | 2.2733E-02 |
| | 1/10 | 2.7203 | 1.7685E-03 | 0.7045 | 3.3373E-03 |
| | 1/16 | 15.1587 | 8.2983E-04 | 3.7406 | 1.3408E-03 |
| | 1/22 | 50.2882 | 5.8791E-04 | 11.7378 | 7.7962E-04 |
| $\frac{1-xyt+\sin(xyt)}{10}$ | 1/4 | 0.0845 | 1.0447E-02 | 0.0325 | 2.2731E-02 |
| | 1/10 | 2.9924 | 1.7737E-03 | 0.7802 | 3.3370E-03 |
| | 1/16 | 17.1431 | 8.0822E-04 | 4.2529 | 1.3406E-03 |
| | 1/22 | 54.7490 | 5.8871E-04 | 13.4222 | 7.7789E-04 |

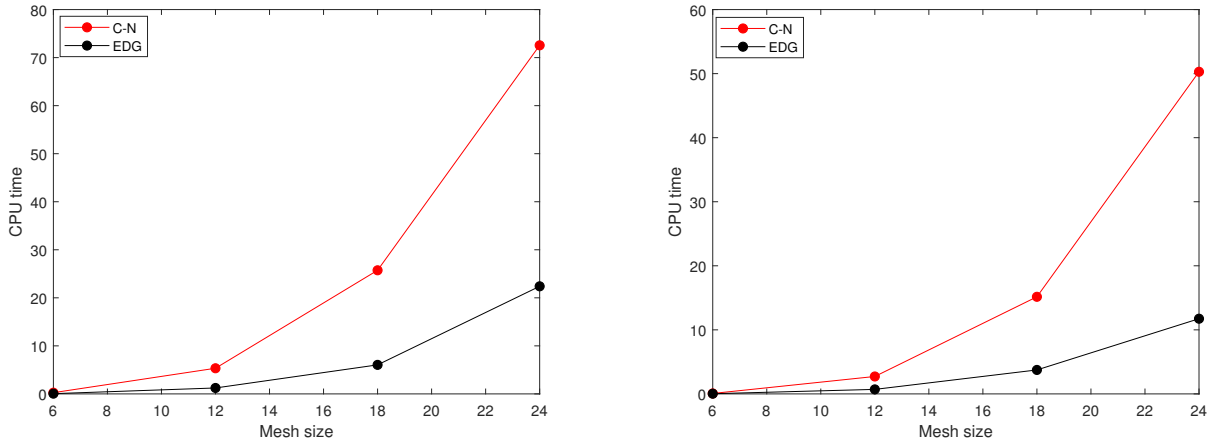


(a) $\alpha(x, y, t) = \frac{e^{xyt}+\cos(xyt)}{30}$ (b) $\alpha(x, y, t) = \frac{5+(xy)^3-(xt)^4}{50}$

**Figure 5.** The CPU time comparison of the C-N and EDG methods for Example 2.

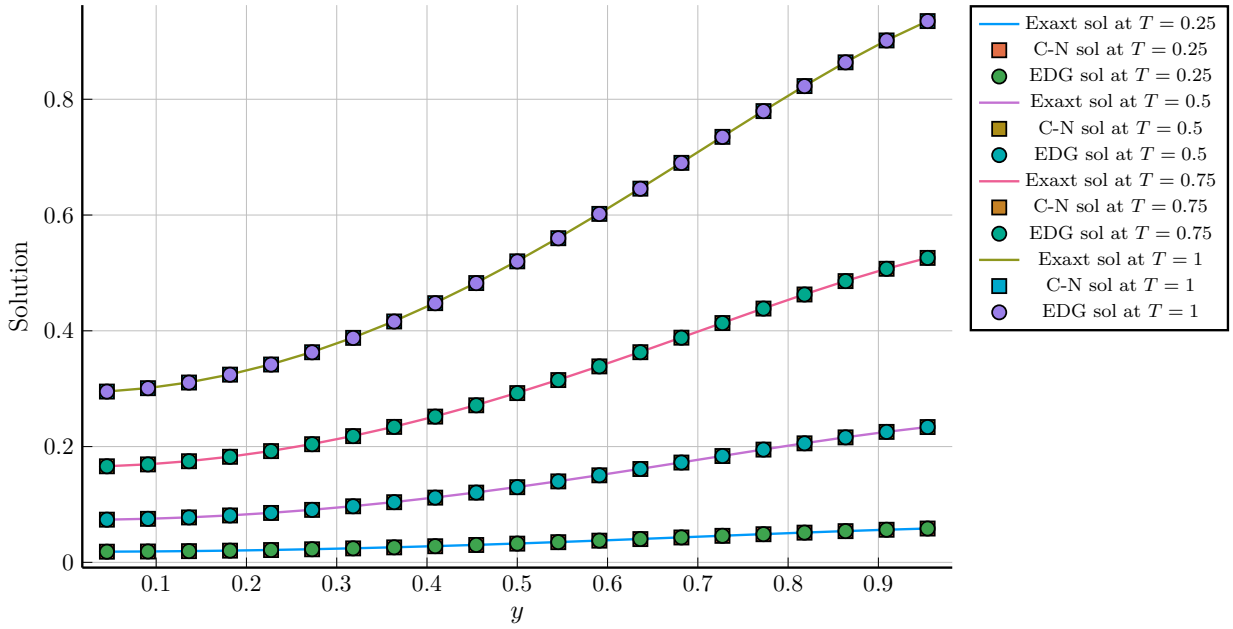


**Figure 6.** Numerical comparison for Example 2 between the exact solution and the numerical solutions obtained using the C-N and EDG methods with $h = 1/22$, $\tau = 0.01$, $x = 0.5$ and $\alpha(x, y, t) = \frac{16-e^{xyt}}{17}$.

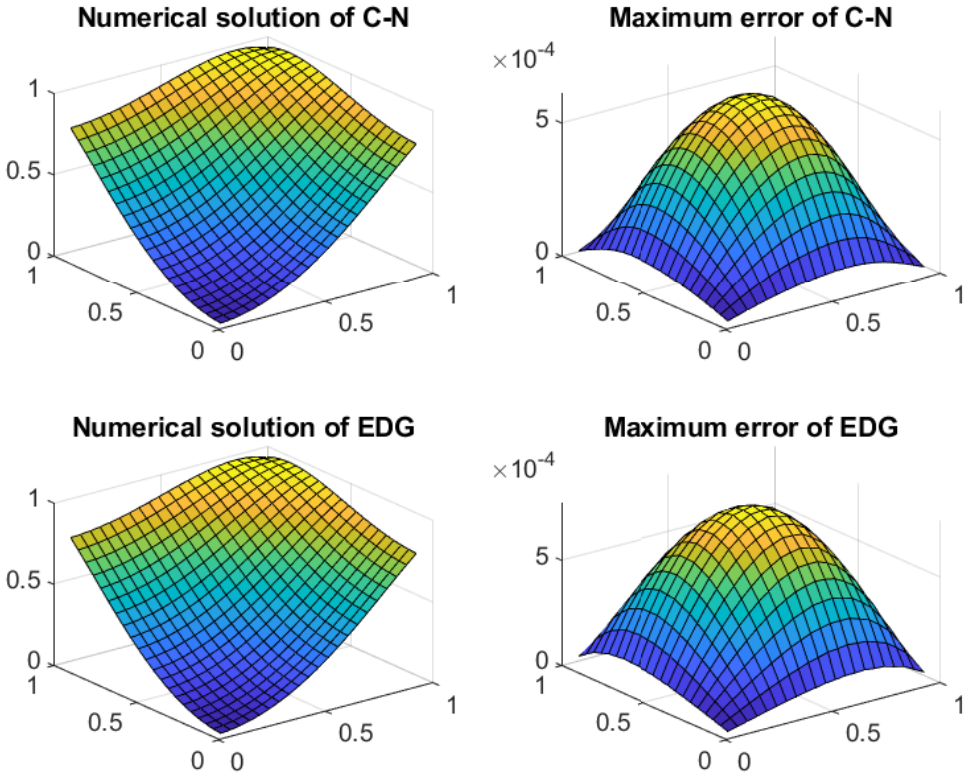


**Figure 7.** The numerical solutions and maximum errors of the C-N and EDG methods with $h = 1/22$, $\tau = 0.01$ and $\alpha(x, y, t) = \frac{3+(xy)^2-(xt)^3}{30}$ for Example 2.

**Example 3.** *Here, the following two-dimensional VO-TFDE is considered:*

$$ {}_0^C D_t^{\alpha(x,y,t)} u(x, y, t) = \frac{\partial^2 u(x, y, t)}{\partial x^2} + \frac{\partial^2 u(x, y, t)}{\partial y^2} + \left( \frac{120 t^{5-a(x,y,t)}}{\Gamma(6 - a(x, y, t))} + \pi^2 t^5 \right) \frac{(\sin(\pi x) + \sin(\pi y))}{2}, $$

with the initial and boundary conditions

$$ \begin{aligned} &u(x, y, 0) = 0, \\ &u(x, 0, t) = \frac{1}{2} t^5 \sin(\pi x), \quad u(x, 1, t) = \frac{1}{2} t^5 \sin(\pi x), \\ &u(0, y, t) = \frac{1}{2} t^5 \sin(\pi y), \quad u(1, y, t) = \frac{1}{2} t^5 \sin(\pi y), \end{aligned} $$

and the exact analytical solution of the following form:

$$ u(x, y, t) = \frac{1}{2} t^5 (\sin(\pi x) + \sin(\pi y)). $$

Table 3 highlights the numerical results of solving Example 3 using CN and EDG methods with $T = 1, \tau = 0.01, h^{-1} = 12, 24$ and different VO functions. From the data in this table, it can be seen that the numerical solutions converge to the exact solution where maximum errors decrease as mesh sizes increase. A reduction of CPU timing and, hence, computational burden is also noted in using the EDG method over the CN method for solving the considered problem. This can be beneficial for capturing the long-term behavior of physical phenomena that is governed by VO fractional models. From the previous discussion, it follows that the proposed methods are accurate and the EDG method is superior to the C-N method in terms of CPU timing. Finally, Table 4 highlights the computational orders of the proposed methods for solving Examples 1–3. From this table, the second order convergence of the proposed methods can be anticipated, which is in line with the theoretical considerations.

**Table 3.** The CPU times and maximum errors for Example 3 at T = 1, $\tau = 0.01$.

| | $h^{-1} = 12$ | | | | $h^{-1} = 24$ | | | |
|---|---|---|---|---|---|---|---|---|
| | C-N | | EDG | | CN | | EDG | |
| $\alpha(x, y, t)$ | CPU time | *MAE* | CPU time | *MAE* | CPU time | *MAE* | CPU time | *MAE* |
| $\frac{10-(xyt)^3}{80}$ | 4.2446 | 2.9811E-03 | 0.9564 | 3.0869E-03 | 57.7629 | 3.7745E-04 | 11.7092 | 5.3877E-04 |
| $5^{yt-3}$ | 5.2871 | 3.0868E-03 | 1.2871 | 3.1129E-03 | 69.0271 | 5.4651E-04 | 16.3071 | 6.8800E-04 |
| $\frac{11-\cos(xt)^2}{11}$ | 1.4539 | 2.4022E-03 | 0.4342 | 2.4534E-03 | 16.7202 | 3.2210E-04 | 5.8109 | 3.1297E-04 |
| $\frac{15+\sin(yt)^5}{16}$ | 2.6672 | 2.4036E-03 | 0.8971 | 2.4604E-03 | 44.4374 | 3.1177E-04 | 8.8679 | 3.1733E-04 |
| $\frac{9-x^5+t^3}{120}$ | 4.0845 | 3.0183E-03 | 1.3774 | 3.1207E-03 | 64.1056 | 4.3822E-04 | 14.0114 | 5.7422E-04 |
| $\frac{15-\sin(xyt)^4}{16}$ | 2.7664 | 2.3978E-03 | 9.95E-01 | 2.4571E-03 | 36.6685 | 3.1184E-04 | 10.6867 | 3.0756E-04 |
| $\frac{1-(xyt)^3+\cos(xyt)^2}{10}$ | 6.5047 | 2.9637E-03 | 1.931 | 3.0515E-03 | 96.8315 | 3.8151E-04 | 24.4635 | 5.2750E-04 |
| $\frac{e^{xyt}+\cos(xyt)}{30}$ | 8.3275 | 3.0230E-03 | 2.3265 | 3.1152E-03 | 125.3629 | 4.5041E-04 | 33.0581 | 5.6177E-04 |
| $\frac{16-e^{xyt}}{17}$ | 1.8139 | 2.3908E-03 | 0.5174 | 2.4595E-03 | 28.0809 | 3.1432E-04 | 6.7689 | 2.5614E-04 |
| $\frac{3+(xy)^2-(xt)^3}{30}$ | 4.2048 | 3.0191E-03 | 1.0323 | 3.0820E-03 | 69.2202 | 4.1416E-04 | 14.2108 | 5.7308E-04 |
| $\frac{5+(xy)^3-(xt)^4}{50}$ | 5.9701 | 3.0114E-03 | 1.5368 | 3.0890E-03 | 86.0504 | 4.0849E-04 | 20.5851 | 5.6393E-04 |
| $\frac{1-xyt+\sin(xyt)}{10}$ | 6.4259 | 3.0110E-03 | 1.4328 | 3.0912E-03 | 74.6506 | 4.0501E-04 | 18.0687 | 5.6381E-04 |

**Table 4.** Computational orders of solving Examples 1–3 at $T = 1$ and $\tau = 0.01$.

| | | | C-N | | EDG | |
|---|---|---|---|---|---|---|
| Example | $\alpha(x, y, t)$ | $h$ | *MAE* | *CO* | *MAE* | *CO* |
| 1 | $\frac{10-(xyt)^3}{80}$ | 1/4 | 9.0598E-03 | | 1.8596E-02 | |
| | | 1/8 | 2.4085E-03 | 1.91 | 3.7500E-03 | 2.31 |
| | | 1/16 | 5.0287E-04 | 2.25 | 8.7401E-04 | 2.10 |
| 2 | $\frac{16-e^{xyt}}{17}$ | 1/4 | 1.0000E-02 | | 2.1580E-02 | |
| | | 1/8 | 2.6132E-03 | 1.93 | 5.0291E-03 | 2.10 |
| | | 1/16 | 7.8225E-04 | 1.74 | 1.2959E-03 | 1.95 |
| 3 | $\frac{11-cos(xt)^2}{11}$ | 1/4 | 2.3825E-02 | | 2.6705E-02 | |
| | | 1/8 | 5.8325E-03 | 2.03 | 6.0067E-03 | 2.15 |
| | | 1/16 | 1.1573E-03 | 2.33 | 1.2173E-03 | 2.30 |

### 6.2. Discussion of results

In the previous subsection, three numerical examples were solved using the proposed methods, and the results were illustrated in Tables 1–3 along with Figures 2–7. In view of the said tables, it can be seen that the numerical solutions of the proposed methods approach the exact solution as the spatial step size decreases. This is in line with our theoretical analysis. In addition, the EDG method was observed to be computationally efficient compared to the C-N method in solving the test problems, where the former required less CPU time compared to the latter. Such reduction in computational burden is attributed to the smaller number of mesh points comprised in the iterative process as discussed earlier. The experimental results are in line with the considerations of previous sections and demonstrate the feasibility, accuracy and efficiency of the proposed methods.

## 7. Conclusions

The VO fractional diffusion equation and its numerical solution are of practical importance for describing complex diffusion processes in which the system memory changes as a function of time and/or space variables. In this paper, the two-dimensional VO-TFDE (1.1) has been considered to account for its numerical solution. A C-N difference scheme along with an EDG method constructed based on a skewed finite difference approximation on the rotated grid have been developed for solving the VO fractional problem. The stability and convergence analyses have been investigated in detail. Numerical test problems were provided to illustrate the capability and performance of the proposed methods.

Based on the numerical simulations and the discussion of experimental results, some conclusions are drawn.

First, both C-N and EDG methods perform well for the VO-TFDE as their numerical solutions are found to be in good agreement with the exact analytical solutions. See Figures 3, 4, 6 and 7.

Second, the proposed methods are stable and convergent, and the maximum absolute errors are observed to decrease as the mesh sizes increase. See Tables 1 and 2.

Third, the EDG method reduces the computational burden of solving the VO-TFDE and results in faster simulations compared to the C-N difference method. See Figures 2 and 5.

Finally, the current work has successfully developed the C-N and EDG numerical methods to solve the fractional diffusion equation involving the VO time derivative defined in section one. The extension of the proposed methods to other classes of linear and nonlinear fractional differential equations with time-invariant type VO derivative [63] is an interesting line of future research. The construction of the proposed methods based on higher-order difference approximations for enhancing the accuracy is another direction for further study.

## Use of AI tools declaration

The authors declare they have not used Artificial Intelligence (AI) tools in the creation of this article.

## Acknowledgments

The authors would like to acknowledge the support provided by the Deanship of Research Oversight and Coordination (DROC) at King Fahd University of Petroleum & Minerals (KFUPM) for funding this work through project (No. EC221011). We are thankful for the anonymous reviewers for their valuable comments and suggestions.

## Conflict of interest

The authors declare no conflicts of interest.

## References

1. O. Nave, Analysis of the two-dimensional polydisperse liquid sprays in a laminar boundary layer flow using the similarity transformation method, *Adv. Model. and Simul. in Eng. Sci.*, **2** (2015), 20. https://doi.org/10.1186/s40323-015-0042-8
2. A. Lozynskyy, A. Chaban, T. Perzynski, A. Szafraniec, L. Kasha, Application of fractional-order calculus to improve the mathematical model of a two-mass system with a long shaft, *Energies*, **14** (2021), 1854. https://doi.org/10.3390/en14071854
3. M. I. Asjad, R. Ali, A. Iqbal, T. Muhammad, Y. M. Chu, Application of water based drilling clay-nanoparticles in heat transfer of fractional maxwell fluid over an infinite flat surface, *Sci. Rep.*, **11** (2021), 18833. https://doi.org/10.1038/s41598-021-98066-w
4. D. Baleanu, A. Fernandez, A. Akgl, On a fractional operator combining proportional and classical differintegrals, *Mathematics*, **8** (2020), 360. https://doi.org/10.3390/math8030360
5. G. Liu, S. Li, J. Wang, New green-ampt model based on fractional derivative and its application in 3d slope stability analysis, *J. Hydrol.*, **603** (2021), 127084. https://doi.org/10.1016/j.jhydrol.2021.127084
6. P. Kumar, V. S. Erturk, R. Banerjee, M. Yavuz, V. Govindaraj, Fractional modeling of plankton-oxygen dynamics under climate change by the application of a recent numerical algorithm, *Phys. Scr.*, **96** (2021), 124044. https://doi.org/10.1088/1402-4896/ac2da7
7. M. Inc, B. Acay, H. W. Berhe, A. Yusuf, A. Khan, S. W. Yao, Analysis of novel fractional COVID-19 model with real-life data application, *Results Phys.*, **23** (2021), 103968. https://doi.org/10.1016/j.rinp.2021.103968
8. W. Y. Shen, Y. M. Chu, M. ur Rahman, I. Mahariq, A. Zeb, Mathematical analysis of hbv and hcv co-infection model under nonsingular fractional order derivative, *Results Phys.*, **28** (2021), 104582. https://doi.org/10.1016/j.rinp.2021.104582
9. I. Podlubny, *Fractional differential equations: an introduction to fractional derivatives, fractional differential equations, to methods of their solution and some of their applications*, New York: Academic Press, 1999.
10. A. A. Kilbas, H. M. Srivastava, J. J. Trujillo, *Theory and applications of fractional differential equations*, Amsterdam: Elsevier Science, 2006.

11. C. Li, F. Zeng, *Numerical methods for fractional calculus*, Boca Raton: CRC Press, 2015.
12. G. S. Teodoro, J. A. T. Machado, E. C. de Oliveira, A review of definitions of fractional derivatives and other operators, *J. Comput. Phys.*, **388** (2019), 195–208. https://doi.org/10.1016/j.jcp.2019.03.008
13. M. D. Ortigueira, J. A. T. Machado, What is a fractional derivative, *J. Comput. Phys.*, **293** (2015), 4–13. https://doi.org/10.1016/j.jcp.2014.07.019
14. V. E. Tarasov, No nonlocality. no fractional derivative, *Commun. Nonlinear Sci.*, **62** (2018), 157–163. https://doi.org/10.1016/j.cnsns.2018.02.019
15. H. G. Sun, W. Chen, H. Wei, Y. Q. Chen, A comparative study of constant-order and variable-order fractional models in characterizing memory property of systems, *Eur. Phys. J. Spec. Top.*, **193** (2011), 185–192. https://doi.org/10.1140/epjst/e2011-01390-6
16. S. G. Samko, B. Ross, Integration and differentiation to a variable fractional order, *Integr. Transf. Spec. F.*, **1** (1993), 277–300. https://doi.org/10.1080/10652469308819027
17. C. F. Lorenzo, T. T. Hartley, Initialization, conceptualization, and application in the generalized (fractional) calculus, *Crit. Rev. Biomed. Eng.*, **35** (2007), 447–553. https://doi.org/10.1615/CritRevBiomedEng.v35.i6.10
18. C. F. Lorenzo, T. T. Hartley, Variable order and distributed order fractional operators, *Nonlinear Dynamics*, **29** (2002), 57–98. https://doi.org/10.1023/A:1016586905654
19. C. F. Coimbra, Mechanics with variable-order differential operators, *Ann. Phys.*, **515** (2003), 692–703. https://doi.org/10.1002/andp.200351511-1203
20. X. Zheng, H. Wang, Optimal-order error estimates of finite element approximations to variable-order time-fractional diffusion equations without regularity assumptions of the true solution, *IMA J. Numer. Anal.*, **41** (2021), 1522–1545. https://doi.org/10.1093/imanum/draa013
21. P. Pandey, J. F. Gomez-Aguilar, On solution of a class of nonlinear variable order fractional reaction-diffusion equation with mittag-effler kernel, *Numer. Meth. Part. D. E.*, **37** (2021), 998–1011. https://doi.org/10.1002/num.22563
22. M. Hosseininia, M. H. Heydari, F. M. M. Ghaini, A numerical method for variable-order fractional version of the coupled 2d burgers equations by the 2D chelyshkov polynomials, *Math. Method. Appl. Sci.*, **44** (2021), 6482–6499. https://doi.org/10.1002/mma.7199
23. H. Hassani, Z. Avazzadeh, J. A. T. Machado, Numerical approach for solving variable-order space-time fractional telegraph equation using transcendental Bernstein series, *Engineering with Computers*, **36** (2020), 867–878. https://doi.org/10.1007/s00366-019-00736-x
24. K. Sadri, H. Aminikhah, An efficient numerical method for solving a class of variable-order fractional mobile-immobile advection-dispersion equations and its convergence analysis, *Chaos Soliton. Fract.*, **146** (2021), 110896. https://doi.org/10.1016/j.chaos.2021.110896
25. M. Hosseininia, M. H. Heydari, C. Cattani, A wavelet method for non-linear variable-order time fractional 2D Schrodinger equation, *Discrete Cont. Dyn.-S*, **14** (2021), 2273–2295. https://doi.org/10.3934/dcdss.2020295
26. M. D. Ortigueira, D. Valerio, J. T. Machado, Variable order fractional systems, *Commun. Nonlinear Sci.*, **71** (2019), 231–243. https://doi.org/10.1016/j.cnsns.2018.12.003

27. H. Wang, X. Zheng, Wellposedness and regularity of the variable-order time-fractional diffusion equations, *J. Math. Anal. Appl.*, **475** (2019), 1778–1802. https://doi.org/10.1016/j.jmaa.2019.03.052

28. R. Almeida, D. Tavares, D. F. M. Torres, *The variable-order fractional calculus of variations*, Heidelberg: Springer, 2019. https://doi.org/10.1007/978-3-319-94006-9

29. N. H. Sweilam, S. M. Al-Mekhlafi, A. O. Albalawi, J. A. T. Machado, Optimal control of variable-order fractional model for delay cancer treatments, *Appl. Math. Model.*, **89** (2021), 1557–1574. https://doi.org/10.1016/j.apm.2020.08.012

30. G. Xiang, D. Yin, R. Meng, C. Cao, Predictive model for stress relaxation behavior of glassy polymers based on variable-order fractional calculus, *Polym. Advan. Technol.*, **32** (2021), 703–713. https://doi.org/10.1002/pat.5123

31. X. Liu, D. Li, C. Han, Y. Shao, A Caputo variable-order fractional damage creep model for sandstone considering effect of relaxation time, *Acta Geotech.*, **17** (2022), 153–167. https://doi.org/10.1007/s11440-021-01230-9

32. W. Fei, L. Jie, Z. Quanle, L. Cunbao, C. Jie, G. Renbo, A triaxial creep model for salt rocks based on variable-order fractional derivative, *Mech. Time-Depend. Mater.*, **25** (2021), 101–118. https://doi.org/10.1007/s11043-020-09470-0

33. H. Jahanshahi, S. S. Sajjadi, S. Bekiros, A. A. Aly, On the development of variable-order fractional hyperchaotic economic system with a nonlinear model predictive controller, *Chaos Soliton. Fract.*, **144** (2021), 110698. https://doi.org/10.1016/j.chaos.2021.110698

34. J. Fan, T. Gu, P. Wang, W. Cai, X. Fan, G. Zhang, Constitutive modeling of sintered nano-silver particles: A variable-order fractional model versus an anand model, *2021 22nd International Conference on Thermal, Mechanical and Multi-Physics Simulation and Experiments in Microelectronics and Microsystems (EuroSimE)*, St. Julian, Malta, 2021, 1–4 https://doi.org/10.1109/EuroSimE52062.2021.9410807

35. S. Patnaik, J. P. Hollkamp, F. Semperlotti, Applications of variable-order fractional operators: a review, *P. Royal Soc. A-Math. Phy.*, **476** (2020), 20190498. https://doi.org/10.1098/rspa.2019.0498

36. H. Sun, A. Chang, Y. Zhang, W. Chen, A review on variable-order fractional differential equations: mathematical foundations, physical models, numerical methods and applications, *Fract. Calc. Appl. Anal.*, **22** (2019), 27–59. https://doi.org/10.1515/fca-2019-0003

37. M. R. S. Ammi, I. Jamiai, D. F. Torres, Finite element approximation for a class of Caputo time-fractional diffusion equations, *Comput. Math. Appl.*, **78** (2019), 1334–1344. https://doi.org/10.1016/j.camwa.2019.05.031

38. B. Li, H. Luo, X. Xie, Analysis of a time-stepping scheme for time fractional diffusion problems with nonsmooth data, *SIAM J. Numer. Anal.*, **57** (2019), 779–798. https://doi.org/10.1137/18M118414X

39. U. Ali, M. Sohail, M. Usman, F. A. Abdullah, I. Khan, K. S. Nisar, Fourth-order difference approximation for time-fractional modified sub-diffusion equation, *Symmetry*, **12** (2020), 691. https://doi.org/10.3390/sym12050691

40. N. H. Tuan, Y. E. Aghdam, H. Jafari, H. Mesgarani, A novel numerical manner for two-dimensional space fractional diffusion equation arising in transport phenomena, *Numer. Meth. Part. D. E.*, **37** (2021), 1397–1406. https://doi.org/10.1002/num.22586

41. F. M. Salama, N. H. M. Ali, Computationally efficient hybrid method for the numerical solution of the 2D time fractional advection-diffusion equation, *Int. J. Math. Eng. Manag.*, **5** (2020), 432–446. https://doi.org/10.33889/IJMEMS.2020.5.3.036

42. N. Dhiman, M. Huntul, M. Tamsir, A modified trigonometric cubic b-spline collocation technique for solving the time-fractional diffusion equation, *Eng. Computation.*, **38** (2021), 2921–2936. https://doi.org/10.1108/EC-06-2020-0327

43. F. M. Salama, N. H. M. Ali, N. N. A. Hamid, Fast $O(N)$ hybrid Laplace transform-finite difference method in solving 2D time fractional diffusion equation, *J. Math. Comput. Sci.*, **23** (2021), 110–123. https://doi.org/10.22436/jmcs.023.02.04

44. F. M. Salama, N. N. A. Hamid, N. H. M. Ali, U. Ali, An efficient modified hybrid explicit group iterative method for the time-fractional diffusion equation in two space dimension, *AIMS Mathematics*, **7** (2022), 2370–2392. https://doi.org/10.3934/math.2022134

45. F. M. Salama, N. N. A. Hamid, U. Ali, N. H. M. Ali, Fast hybrid explicit group methods for solving 2d fractional advection-diffusion equation, *AIMS Mathematics*, **7** (2022), 15854–15880. https://doi.org/10.3934/math.2022868

46. M. A. Khan, N. Alias, U. Ali, A new fourth-order grouping iterative method for the time fractional sub-diffusion equation having a weak singularity at initial time, *AIMS Mathematics*, **8** (2023), 3725–13746. https://doi.org/10.3934/math.2023697

47. U. Ali, M. Sohail, F. A. Abdullah, An efficient numerical scheme for variable-order fractional sub-diffusion equation, *Symmetry*, **12** (2020), 1437. https://doi.org/10.3390/sym12091437

48. F. R. Lin, Q. Y. Wang, X. Q. Jin, Crank-Nicolson-Weighted-Shifted-Grunwald-difference schemes for space riesz variable-order fractional diffusion equations, *Numer. Algor.*, **87** (2021), 601–631. https://doi.org/10.1007/s11075-020-00980-z

49. U. Ali, M. Naeem, F. A. Abdullah, M. K. Wang, F. M. Salama, Analysis and implementation of numerical scheme for the variable-order fractional modified sub-diffusion equation, *Fractals*, **30** (2022), 2240253. https://doi.org/10.1142/S0218348X22402538

50. J. Jia, H. Wang, X. Zheng, A preconditioned fast finite element approximation to variable-order time-fractional diffusion equations in multiple space dimension, *Appl. Numer. Math.*, **163** (2021), 15–29. https://doi.org/10.1016/j.apnum.2021.01.001

51. M. H. Heydari, Z. Avazzadeh, M. F. Haromi, A wavelet approach for solving multi-term variable-order time fractional diffusion-wave equation, *Appl. Math. Comput.*, **341** (2019), 215–228. https://doi.org/10.1016/j.amc.2018.08.034

52. S. Wei, W. Chen, Y. Zhang, H. Wei, R. M. Garrard, A local radial basis function collocation method to solve the variable-order time fractional diffusion equation in a two-dimensional irregular domain, *Numer. Meth. Part. D. E.*, **34** (2018), 1209–1223. https://doi.org/10.1002/num.22253

53. J. Jia, H. Wang, X. Zheng, A fast collocation approximation to a two-sided variable-order space-fractional diffusion equation and its analysis, *J. Comput. Appl. Math.*, **388** (2021), 13234. https://doi.org/10.1016/j.cam.2020.113234

54. X. Y. Li, B. Y. Wu, Iterative reproducing kernel method for nonlinear variable-order space fractional diffusion equations, *Int. J. Comput. Math.*, **95** (2018), 1210–1221. https://doi.org/10.1080/00207160.2017.1398325

55. F. M. Salama, N. H. M. Ali, N. N. A. Hamid, Efficient hybrid group iterative methods in the solution of two-dimensional time fractional cable equation, *Adv. Differ. Equ.*, **2020** (2020), 257. https://doi.org/10.1186/s13662-020-02717-7

56. M. A. Khan, N. H. M. Ali, N. N. A. Hamid, A new fourth-order explicit group method in the solution of two-dimensional fractional rayleigh-stokes problem for a heated generalized second-grade fluid, *Adv. Differ. Equ.*, **2020** (2020), 598. https://doi.org/10.1186/s13662-020-03061-6

57. A. Ali, T. Abdeljawad, A. Iqbal, T. Akram, M. Abbas, On unconditionally stable new modified fractional group iterative scheme for the solution of 2D time-fractional telegraph model, *Symmetry*, **13** (2021), 2078. https://doi.org/10.3390/sym13112078

58. F. M. Salama, A. T. Balasim, U. Ali, M. A. Khan, Efficient numerical simulations based on an explicit group approach for the time fractional advection-diffusion reaction equation, *Comput. Appl. Math.*, **42** (2023), 157. https://doi.org/10.1007/s40314-023-02278-x

59. N. Abdi, H. Aminikhah, A. H. R. Sheikhani, On rotated grid point iterative method for solving 2d fractional reaction-subdiffusion equation with Caputo-Fabrizio operator, *J. Differ. Equ. Appl.*, **27** (2021), 1134–1160. https://doi.org/10.1080/10236198.2021.1965592

60. F. M. Salama, U. Ali, A. Ali, Numerical solution of two-dimensional time fractional mobile/immobile equation using explicit group methods, *Int. J. Appl. Comput. Math.*, **8** (2022), 188. https://doi.org/10.1007/s40819-022-01408-z

61. Z. Liu, X. Li, A Crank-Nicolson difference scheme for the time variable fractional mobile-immobile advection-dispersion equation, *J. Appl. Math. Comput.*, **56** (2018), 391–410. https://doi.org/10.1007/s12190-016-1079-7

62. A. R. Abdullah, The four point explicit decoupled group (EDG) method: A fast Poisson solver, *Int. J. Comput. Math.*, **38** (1991), 61–70. https://doi.org/10.1080/00207169108803958

63. X. M. Gu, H. W. Sun, Y. L. Zhao, X. Zheng, An implicit difference scheme for time-fractional diffusion equations with a time-invariant type variable order, *Appl. Math. Lett.*, **120** (2021), 107270. https://doi.org/10.1016/j.aml.2021.107270


AIMS Press